



Calhoun: The NPS Institutional Archive
DSpace Repository

NPS Scholarship

Theses

1965

Ultrasonic attenuation in superconducting zinc

Goncz, Joseph P.

Monterey, California: U.S. Naval Postgraduate School

<https://hdl.handle.net/10945/13329>

This publication is a work of the U.S. Government as defined in Title 17, United States Code, Section 101. Copyright protection is not available for this work in the United States.

Downloaded from NPS Archive: Calhoun



Calhoun is the Naval Postgraduate School's public access digital repository for research materials and institutional publications created by the NPS community. Calhoun is named for Professor of Mathematics Guy K. Calhoun, NPS's first appointed -- and published -- scholarly author.

Dudley Knox Library / Naval Postgraduate School
411 Dyer Road / 1 University Circle
Monterey, California USA 93943

<http://www.nps.edu/library>

NPS ARCHIVE
1965
GONCZ, J.

**ULTRASONIC ATTENUATION IN
SUPERCONDUCTING ZINC**

JOSEPH P. GONCZ

U.S. NAVY
MONTEREY, CALIFORNIA

DUDLEY KNOX LIBRARY
NAVAL POSTGRADUATE SCHOOL
MONTEREY CA 93943-5101

ULTRASONIC ATTENUATION IN
SUPERCONDUCTING ZINC

* * * * *

Joseph P. Goncz

ULTRASONIC ATTENUATION IN
SUPERCONDUCTING ZINC

by

Joseph P. Goncz
Captain, United States Army

Submitted in partial fulfillment of
the requirements for the degree of

MASTER OF SCIENCE
IN
PHYSICS

United States Naval Postgraduate School
Monterey, California

1 9 6 5

MS Archive
1965
GONGE, J

~~6E47~~

ULTRASONIC ATTENUATION IN
SUPERCONDUCTING ZINC

by

Joseph P. Goncz

This work is accepted as fulfilling
the thesis requirements for the degree of

MASTER OF SCIENCE

IN

PHYSICS

from the

United States Naval Postgraduate School

ACKNOWLEDGEMENTS

I wish to thank Professor John R. Neighbours for his enthusiastic guidance and patient assistance in conducting the experiment. I also wish to express my appreciation to Mr. Lynwood F. May, USNPGS, who built the He³ cryostat, for his assistance and also to Lt. David Dickmann, USN, who wrote the computer programs.

ABSTRACT

Measurements of the ultrasonic attenuation of 10 and 30 Mcs/sec longitudinal waves by pulsed-echo techniques were made on a 99.999% pure single crystal of superconducting zinc in the $[0001]$ direction as a function of temperature from 4.2°K to 0.320°K using an open-ended type He^3 cryostat. The attenuation was found to be frequency dependent and decreased less sharply near the superconducting transition temperature, T_c , than predicted by the Bardeen-Cooper-Schrieffer (BCS) theory. Attenuation due to electron-phonon interactions only was found by subtracting from experimental points the value of residual attenuation gotten by extrapolation of the data to $T = 0^{\circ}\text{K}$. Using the BCS theory the zero degree superconducting energy gap was found to be $2 \epsilon(0) = (3.36 \pm 0.13)kT_c$ with $T_c = 0.817^{\circ}\text{K}$.

TABLE OF CONTENTS

	Page
Introduction	1
Experimental Procedures	4
Experimental Results	10
Discussion of Results	26
Appendix I Data Analysis	30
Appendix II Computer Program RESATT	34
Appendix III Computer Program VARIGAP	45
Appendix IV Computer Program ZEROGAP	54
Appendix V Computer Program AVERGAP	77
References	85

LIST OF ILLUSTRATIONS

Figure	Page
1. Ultrasonic Pulsing Equipment Schematic	6
2. Helium 3 Refrigerator Schematic	8
3. Reduced Attenuation vs Reduced Temperature, $\alpha_o = 0.310$ db/cm	11
4. Reduced Attenuation vs Reduced Temperature, $\alpha_o = 0.320$ db/cm	12
5. Reduced Attenuation vs Reduced Temperature, $\alpha_o = 0.330$ db/cm	13
6. $Y = 1/\ln(2/\alpha^*-1)$ vs Reduced Temperature, $\alpha_o = 0.310$ db/cm	14
7. $Y = 1/\ln(2/\alpha^*-1)$ vs Reduced Temperature, $\alpha_o = 0.320$ db/cm	15
8. $Y = 1/\ln(2/\alpha^*-1)$ vs Reduced Temperature, $\alpha_o = 0.330$ db/cm	16
9. Reduced Attenuation vs Reduced Temperature, $\alpha_o = 0.320$ db/cm, BCS Curve for $2 \epsilon(0) = 3.48kT_c$	17
10. Reduced Attenuation vs Reduced Temperature, $\alpha_o = 0.320$ db/cm, BCS Curve for $2 \epsilon(0) = 3.58kT_c$	18
11. Reduced Attenuation vs Reduced Temperature, $\alpha_o = 0.320$ db/cm, BCS Curve for $2 \epsilon(0) = 3.68kT_c$	19
12. $Y = 1/\ln(2/\alpha^*-1)$ vs Reduced Temperature, $\alpha_o = 0.320$ db/cm, BCS Curve for $2 \epsilon(0) = 3.48kT_c$	20
13. $Y = 1/\ln(2/\alpha^*-1)$ vs Reduced Temperature, $\alpha_o = 0.320$ db/cm, BCS Curve for $2 \epsilon(0) = 3.58kT_c$	21
14. $Y = 1/\ln(2/\alpha^*-1)$ vs Reduced Temperature, $\alpha_o = 0.320$ db/cm, BCS Curve for $2 \epsilon(0) = 3.68kT_c$	22
15-26. Graphical Results of Program ZEROGAP	59-70

LIST OF TABLES

Table		Page
I	Result of RESATT Computations	25
II	Zero Degree Energy Gap in Superconducting Zinc	27
III	Comparison of ZEROGAP and RESATT Results	58
IV	Summary of Computer Calculations	78

INTRODUCTION

The rapid decrease in the attenuation of ultrasonic waves in superconductors below the superconducting transition temperature, T_c , was first observed by Bömmel and Mackinnon.^{1,2} Bömmel investigated the ultrasonic attenuation of shear and longitudinal waves in a cylindrical crystal of lead in the frequency range from 9-27 Mc/sec from approximately 18°K to 1.5°K. He found a marked decrease in the attenuation in the superconducting state which was frequency dependent. No theoretical explanation was made, though he suggested that the results might lend support to the idea that superconductivity is due mainly to interactions between electrons and lattice vibrations. Mackinnon investigated the absorption of 10 Mc/sec sound pulses in a superconducting polycrystalline tin rod and in a polycrystalline magnesium rod between 1.5°K and 4.2°K. In tin he found the attenuation decreased by a factor of about 50 and in magnesium that the attenuation decreased steadily with decreasing temperature.

This decrease in the electron contribution to the ultrasonic attenuation was first satisfactorily explained in 1957 by the theory of Bardeen, Cooper, and Schrieffer (BCS theory).³ The BCS theory predicts that the ratio of the electron contribution to the attenuation in the superconducting state, α_s , to that in the normal state, α_n , is

$$\frac{\alpha_s}{\alpha_n} = \frac{2}{\exp \left[\frac{\epsilon(T)}{k_B T} \right] + 1},$$

where $2\epsilon(T)$ is the temperature dependent energy gap. The theory further predicts that as T approaches zero, the energy gap approaches $3.50 kT_c$.

Morse and Bohm⁴ were the first to apply this theory to the analysis of ultrasonic attenuation data on tin and indium, shortly before the publication of the BCS theory, basing their analysis on a conversation

with Professor Bardeen. Their analysis pointed out the remarkable agreement between the BCS theory and their experimental data. Since then the BCS theory has been applied to many superconducting metals.^{5,6}

These investigations have all shown close agreement between the theory and experiment, but have also indicated the need for refinement of some of the simplifying assumptions of the BCS theory. The theory shows that the basic interaction causing superconductivity is that of the exchange of a virtual phonon between two electrons. An electron moving through the lattice creates a virtual phonon which is absorbed by a nearby electron. If the distortion of the lattice is such as to surround the electron by a positive charge greater than the electronic one, the second electron sees an attractive potential greater than the repulsive Coulomb one and is attracted. These electrons form what is known as Cooper pairs. The theory then shows that the lowest energy of the system is achieved by the maximum pairing of electrons of opposite spin such that their momenta add to zero. The difference in the normal ground state energy and the superconducting ground state energy is due entirely to an interaction potential, less than zero, arising from the correlation between the Cooper pairs. The energy of this interaction leading to the scattering of one pair to another is the difference between the energy of interaction by means of a phonon and the energy of Coulomb interaction.

The existence of an energy gap then follows from the small, but finite, amount of energy required to break up a Cooper pair. But more important, having a single unpaired electron removes a large number of pairs which could have occupied the state of a Cooper pair. This gap will be temperature dependent since increasing numbers of pairs will be broken up by thermal excitation as the temperature rises from 0°K to T_c .

Morse, Olsen, and Gavenda⁷ pointed out the need to consider the anisotropy of the energy gap and showed that in tin there is considerable

anisotropy ($3.2 kT_c - 4.32 kT_c$). In order to conserve both momentum and energy in a phonon-electron interaction, the component of the electronic velocity parallel to the direction of sound must equal the phonon velocity; i.e., the sound velocity. Since the velocity of electrons at the Fermi surface is in general much greater than that of sound, only those electrons moving at essentially right angles to the direction of sound propagation can interact with the phonons. On the Fermi surface these electrons lie in a narrow band perpendicular to the sound velocity. Since the ultrasonic attenuation in a particular direction is an average over this narrow band, the energy gap measured will be an average for the electrons lying within the band. Anisotropies in the Fermi surface will then lead to anisotropies in the energy gap. The BCS theory makes the simplifying assumption that the interaction energy is isotropic and constant near the Fermi surface. It is this assumption that leads to the BCS prediction that the zero degree energy gap is the same for all superconductors and is equal to $3.5 kT_c$.

The relation for the ratio of ultrasonic attenuation in the superconducting state to that in the normal state follows from the coherence of paired electrons. In the normal state scattering of an electron to another state is independent of any other transitions. However, the pairing of electrons in the superconducting state makes these transitions interdependent and the theory shows that the scattering by pairs is destructive. Thus, the absorption of phonons, causing ultrasonic attenuation, decreases sharply below T_c . With the assumption of low energy phonons; i.e., $\hbar\omega \ll 2\epsilon(0)$, the ratio α_s/α_n follows.

The present work on zinc, which has a hexagonal crystal structure, was undertaken to determine the energy gap in the direction of the c-axis and to compare the results with measurements made in the base plane. Ultrasonic frequencies on the order of 10^7 cps were used, well satisfying the condition for the given expression of α_s/α_n .

EXPERIMENTAL PROCEDURES

A cylindrical, single crystal of zinc, approximately $2\frac{1}{2}$ " long and $\frac{3}{4}$ " in diameter with the c-axis, [0001] direction, parallel to the cylinder axis was purchased from Semi-Elements, Inc. The purity of the sample was stated to be in excess of 99.999%. From this ingot the experimental sample was prepared to the approximate desired size, limited by the cryostat, by cleaving both ends and etching. The ingot was held in a styrofoam form, immersed in liquid nitrogen and cleaved by laying a new, sharp, razor blade at the desired point and rapping it with a mallet. To reduce the diameter, the ends were coated with brushing lacquer and the ingot etched in dilute HCl acid.

Standard ultrasonic pulse-echo techniques⁵ were used and will be discussed only in terms of the experiment. The success of this method depends strongly on having the end faces of the sample flat, parallel, and perpendicular to the direction in the crystal one wishes to investigate. To achieve this, the zinc sample was cast with a cerro-alloy in a bored out, cylindrical jig whose faces were machined flat, parallel and perpendicular to the crystal axis to a tolerance of 0.003". The ends were first lapped on metallographic paper and then polished on a diamond dust wheel.

The final sample was (3.1602 ± 0.0002) cm long and approximately $\frac{5}{8}$ " in diameter at room temperature. A Laue back reflection pattern of the zinc crystal showed concentric circles, indicating a thin polycrystalline layer on each end. However, the x-ray spots showing through the circles indicated that the faces were perpendicular to the c-axis.

A $\frac{1}{2}$ ", X-cut, 10 megacycle quartz transducer was next bonded to the zinc sample. The success of this bond is a critical step in the experimental procedure. After some experimenting, the following procedure proved to be reliable. Both the quartz and sample faces are cleaned first with acetone to remove greasy substances, second with alcohol to remove

water, and finally with acetone to ensure the surfaces are dry. The best bonds were obtained on days when the humidity was low. Next a very small amount of analytical grade glycerin was applied to the zinc and the transducer centered and squeezed to make the glycerin flow and also to remove air bubbles. Glycerin proved to be the most satisfactory bonding material, though its use required the making of a new bond for each run. The critical temperature for the bond was from 40°K to 50°K . If the bond held on being cooled through this range; the bond was good for the run. However, as can be seen, one has already started to cool with He^4 and if the run must be stopped for a broken bond, the delay is both costly and time consuming.

A schematic for the ultrasonic pulsing equipment is shown in Fig. 1. Radio frequency pulses (10 Mcs/sec and 30 Mcs/sec) of approximately two microseconds' duration were generated by an Arenberg Pulsed Oscillator triggered by a Time Mark Generator with a repetition rate of 1000 cps or 100 cps. The slower rate had to be used below 0.5°K to reduce heating of the sample. The rf electrical pulses were simultaneously fed to a Type RM 45A Tektronix Oscilloscope, externally triggered by the Time Mark Generator, and impressed across the piezoelectric quartz transducer. The zinc furnished the rf ground and the oscillator, tuned to the fundamental or odd harmonic of the transducer, caused it to vibrate and send sound waves through the zinc. The sound waves reflected off the other end return to the transducer to produce a voltage across the electrodes furnishing the initial pulse and also to be reflected back through the sample. With a pulse rate of 1000 cps, these reflected echoes had adequate time to decay away between pulses. The voltage produced by each returning echo was amplified and displayed in proper time relation to the initial pulse on the oscilloscope. The change in height of each echo is a measure of the attenuation in the sample due to phonon-electron interaction, impurities, imperfections and in the transducer bonding system. Absolute attenuations are gotten by taking pictures of the scope traces with a Polaroid Oscilloscope Camera, Model 196A, Special, using

ULTRASONIC PULSING EQUIPMENT SCHEMATIC

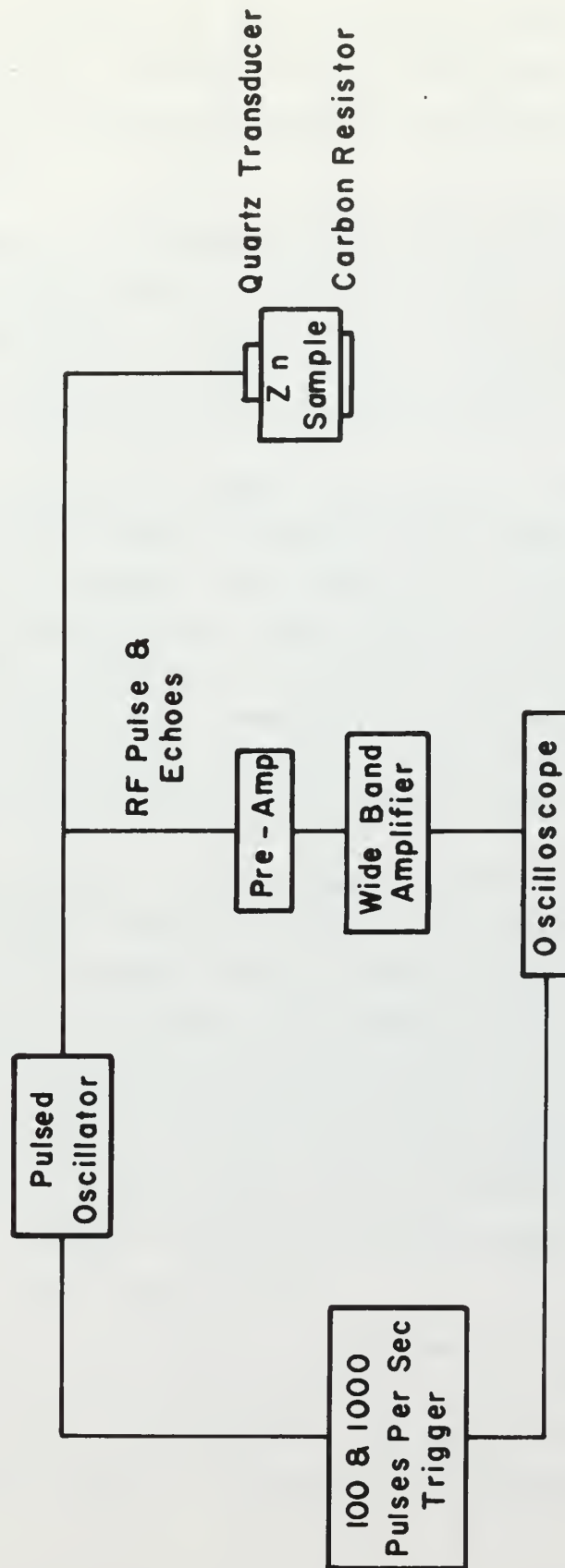


Fig. 1

3000 speed/Type 47A Polaroid film and plotting echo heights vs echo number on semi-log paper. Attenuation effects other than those due to phonon-electron interactions are subtracted off as discussed in the treatment of the data.

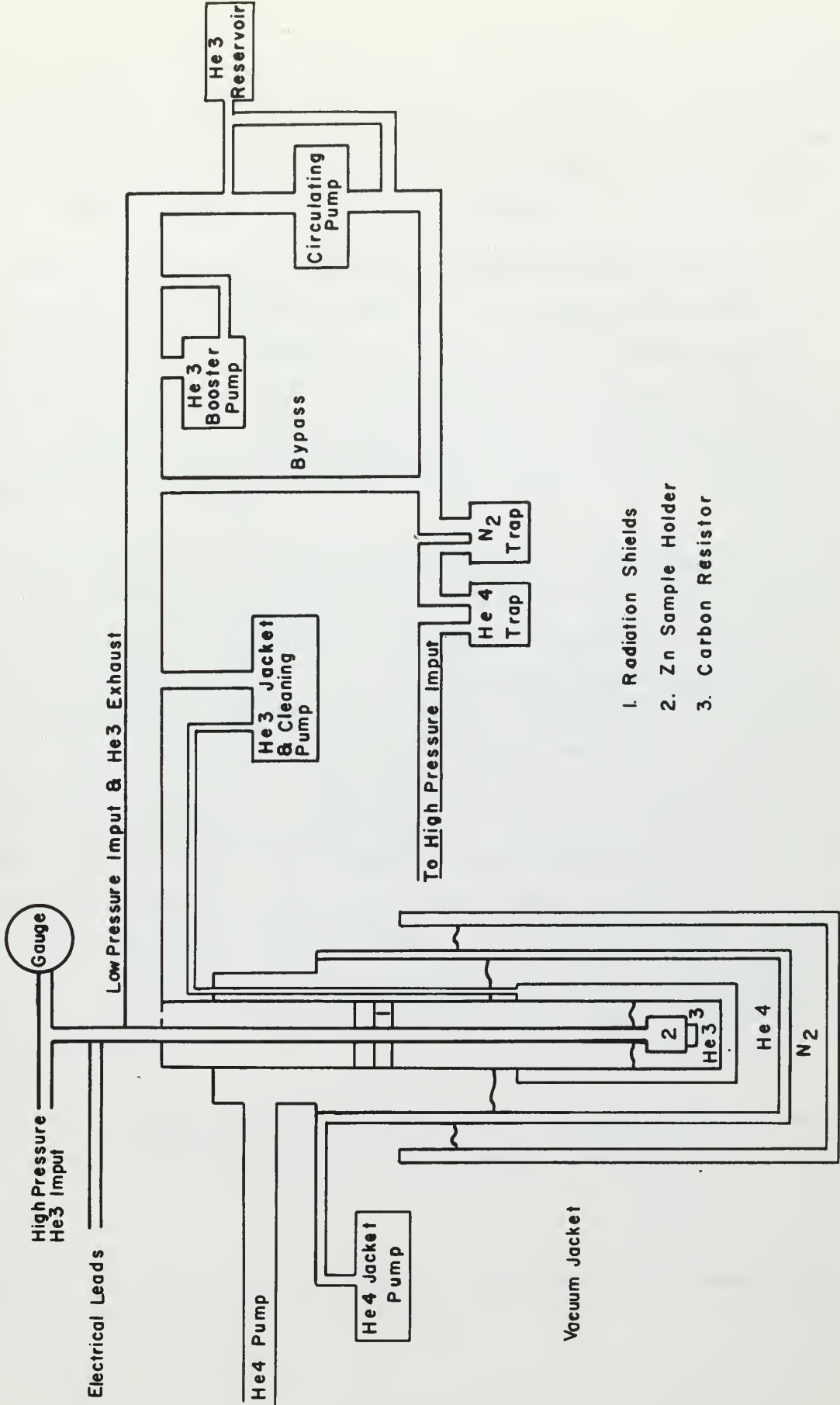
Data were taken in the temperature range from 4.2°K to approximately 0.320°K . The temperature range was obtained in a He^3 cryostat of the open-ended type, a schematic of which is shown in Fig. 2. It is desirable to cool the sample as fast as possible to reduce cooling time, but this is tempered by the necessity of not straining the bond.

The sample was loaded in a copper sample holder, inserted in the He^3 cryostat and the He^3 chamber flushed with dry nitrogen and left at one atmosphere of dry nitrogen. The vacuum jackets of the He^3 cryostat and the He^4 dewar were thoroughly flushed with dry nitrogen and left soft at approximately 300 microns dry nitrogen pressure. The He^4 dewar was also flushed and left at one atmosphere dry nitrogen pressure. The nitrogen dewar was then filled with liquid nitrogen and the whole system cooled to approximately 77°K which takes about six hours.

The He^3 and He^4 jackets were then pumped out until the pressure was less than 5×10^{-6} mm Hg. Keeping the pressure less than this in the He^3 jacket was essential to prevent thermal conduction at the lowest temperatures. While this was being done, the nitrogen and He^4 traps were filled and the He^3 gas circulated for approximately one-half hour to condense out all impurities except He^4 . This was found to be necessary as impurities would freeze out in the cryostat and around the sample holder causing throttling when pumping full out on the He^3 . The He^4 impurity caused no trouble as thermometry was done using a carbon resistor and not by using the He^3 vapor pressure.

When the jackets were pumped out and the He^3 purified, the He^4 dewar was filled and about eight mm Hg of He^3 let into the cryostat; the remainder being returned to the reservoir. The system was then cooled to 4.2°K , taking about 12 hours. The process could be accelerated by

HELIUM 3 REFRIGERATOR SCHEMATIC



- 1. Radiation Shields
- 2. Zn Sample Holder
- 3. Carbon Resistor

Fig. 2

softening the He³ jacket with He⁴. However, achieving a satisfactory vacuum after the system was cooled down was very difficult since helium at that temperature is very difficult to pump. Without a good vacuum the low temperatures desired could not be reached.

Once 4.2°K was reached, the He⁴ was pumped on and the He³ let into the cryostat. A minimum temperature of 1.09°K can be reached this way, well below the temperature at which He³ at one atmosphere will condense; i.e., 3.195°K. When equilibrium was reached, the circulating pump was valved off to pump on the He³. At 500 microns the booster pump was cut in and pumping full out on the He³ the lowest temperatures were reached.

Temperatures were determined by measuring the resistance of a ½-watt Speer Carbon Resistor, nominal resistance 470 ohms, 10%, grade 1002, in a Wheatstone Bridge Circuit employing a lock-in amplifier to measure the bridge unbalance. The resistor was calibrated against the vapor pressure of He⁴ down to 1.1°K using the "1958 He⁴ Scale of Temperature". Down to the lowest temperature reached, the resistor was calibrated against the magnetic susceptibility of cerium magnesium double nitrate (CMN), Ce₃Mg₃(NO₃)₁₂·24H₂O using a Cryotonics Mutual Inductance Bridge.⁸ The susceptibility of CMN is strongly anisotropic with the susceptibility parallel to the symmetry axis essentially zero. To obviate the necessity of packing single crystals, powdered CMN was used. The effective susceptibility is then approximately 65% of the value perpendicular to the symmetry axis, but the gain in the packing fraction offsets this decrease.

Since the temperature dependent part of the susceptibility of CMN perpendicular to the symmetry axis follows Curie's Law

$$\chi \propto \frac{C}{T}$$

the mutual inductance bridge readings are correlated to the temperature and thereby calibrating the carbon resistor.

EXPERIMENTAL RESULTS

Measurements of the ultrasonic attenuation of 10 and 30 Mcs/sec longitudinal waves were made in the [0001] direction on a single crystal of zinc whose ends were slightly polycrystalline. Data were taken in the temperature range 4.2°K to approximately 0.320°K and in the earth's magnetic field. The superconducting transition temperature was determined to be $T_c = 0.817^\circ\text{K}$ and the zero degree superconducting energy gap was measured as $(3.36 \pm 0.13)kT_c$.

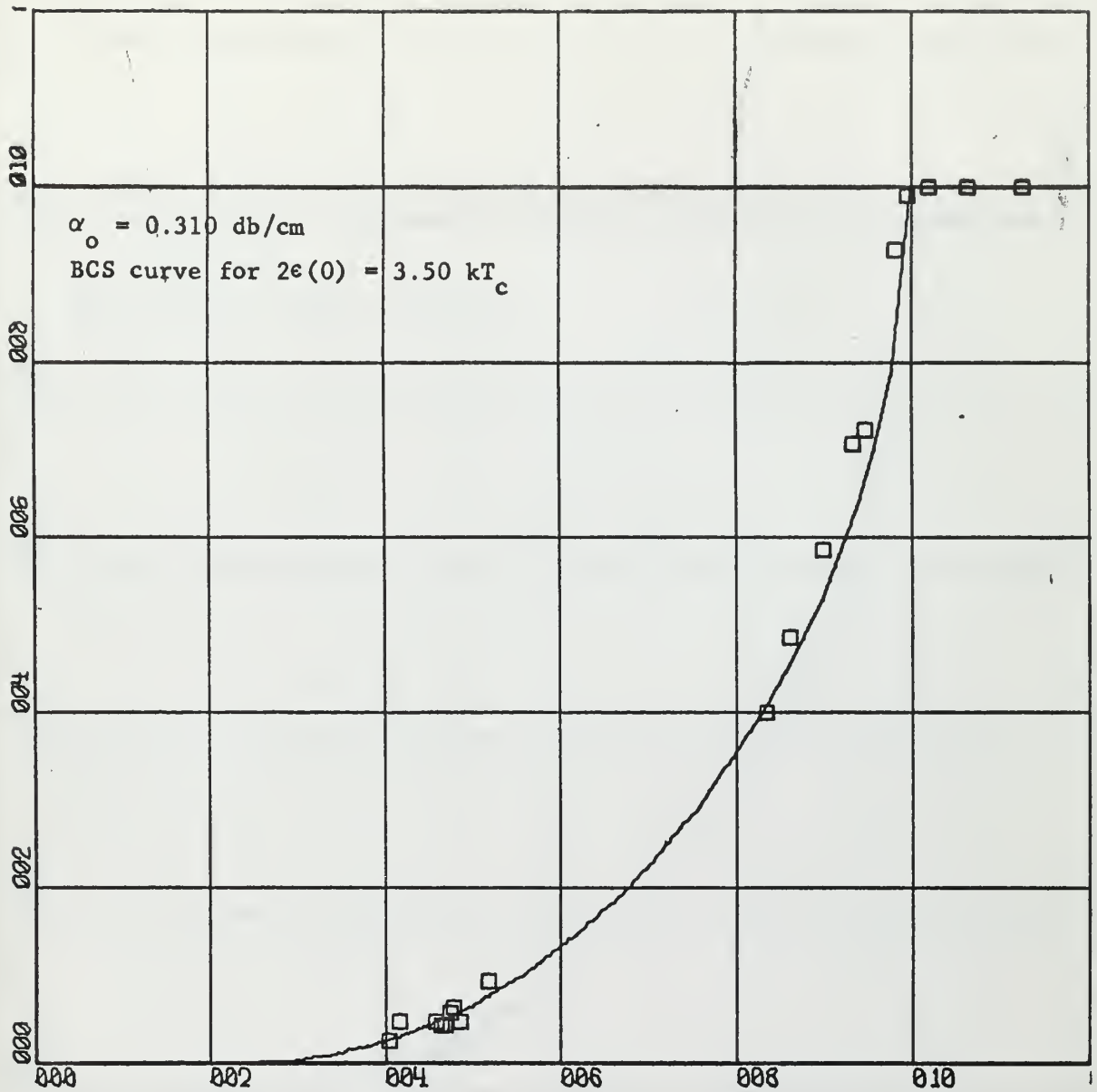
To measure the attenuation as a function of temperature, pictures of echo trains were taken at different temperatures and the heights of the echoes plotted on semi-log paper to obtain the attenuation in units of attenuation per echo. These were plotted as a function of temperature and when extrapolated to $T = 0^\circ\text{K}$ gave an estimate of the residual attenuation. Subtracting the residual attenuation from experimental points gave the attenuation due solely to electron-phonon interactions. These data were then analyzed using the BCS function for reduced attenuation vs reduced temperature

$$\alpha^* = \frac{2}{\exp\left[\frac{\epsilon(T)}{kT}\right] + 1}$$

The details of all these analyses are given in Appendices I - III. In order to illustrate the methods, Figs. 3-14 graphically display the results for one set of data; those of 13 November 1964.

After the transition temperature was determined and an estimate of the residual attenuation made, computer program RESATT was used to determine the residual attenuation and the zero degree energy gap. Figs. 3-5 show the point plots of reduced attenuation vs reduced temperature for three slightly different values of residual attenuation subtracted from the experimental data. By inverting the BCS expression the following function Y is defined:

$$Y = 1/\ln(2/\alpha^* - 1) = (kT_c/\epsilon(t))t.$$

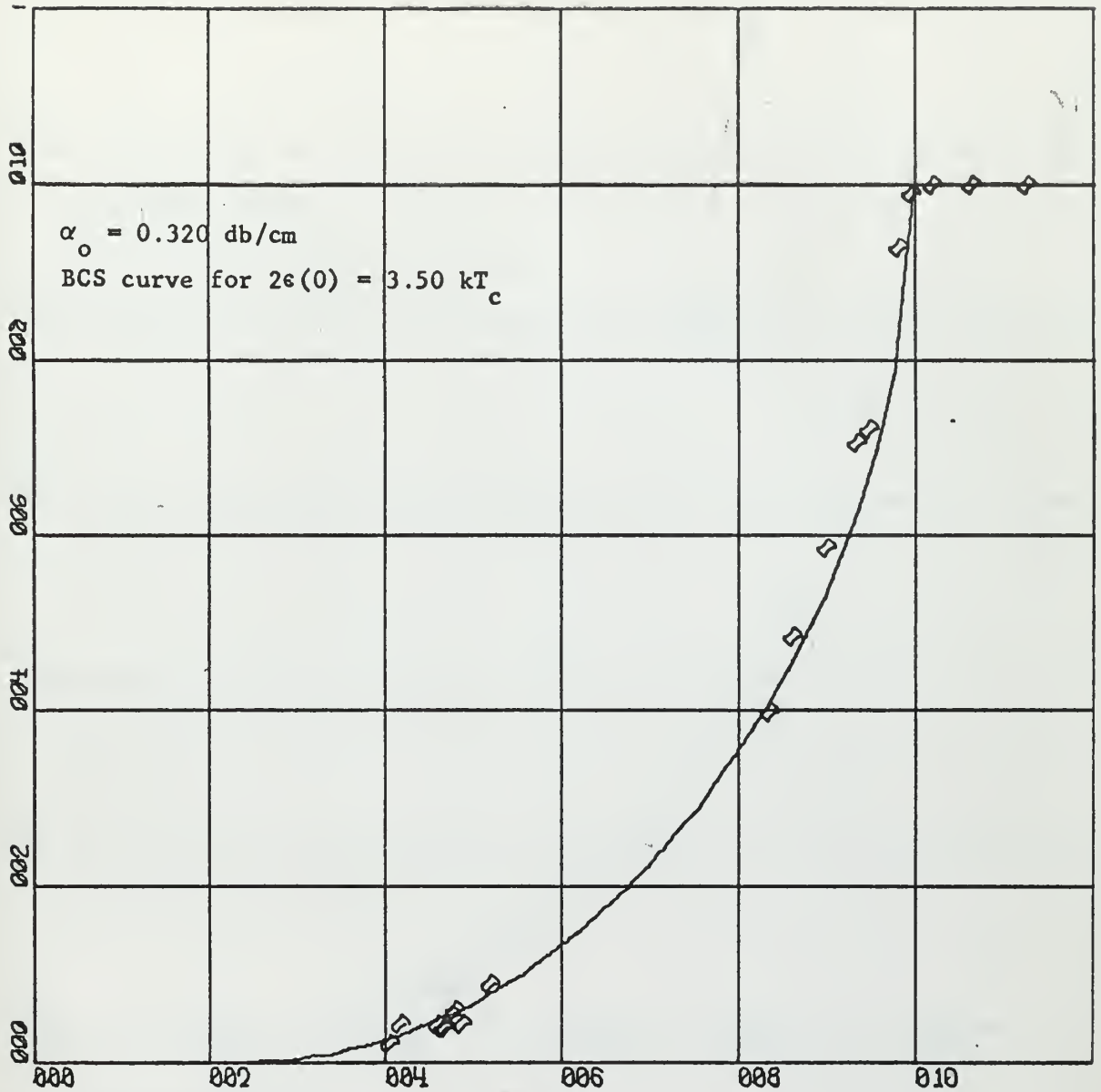


X-SCALE = 2.00E-01 UNITS/INCH

Y-SCALE = 2.00E-01 UNITS/INCH

GONCZ PROJECT 0321 13 NOV 64 30MCS
 REDUCED ATTENUATION VS REDUCED TEMPERATURE

Fig. 3



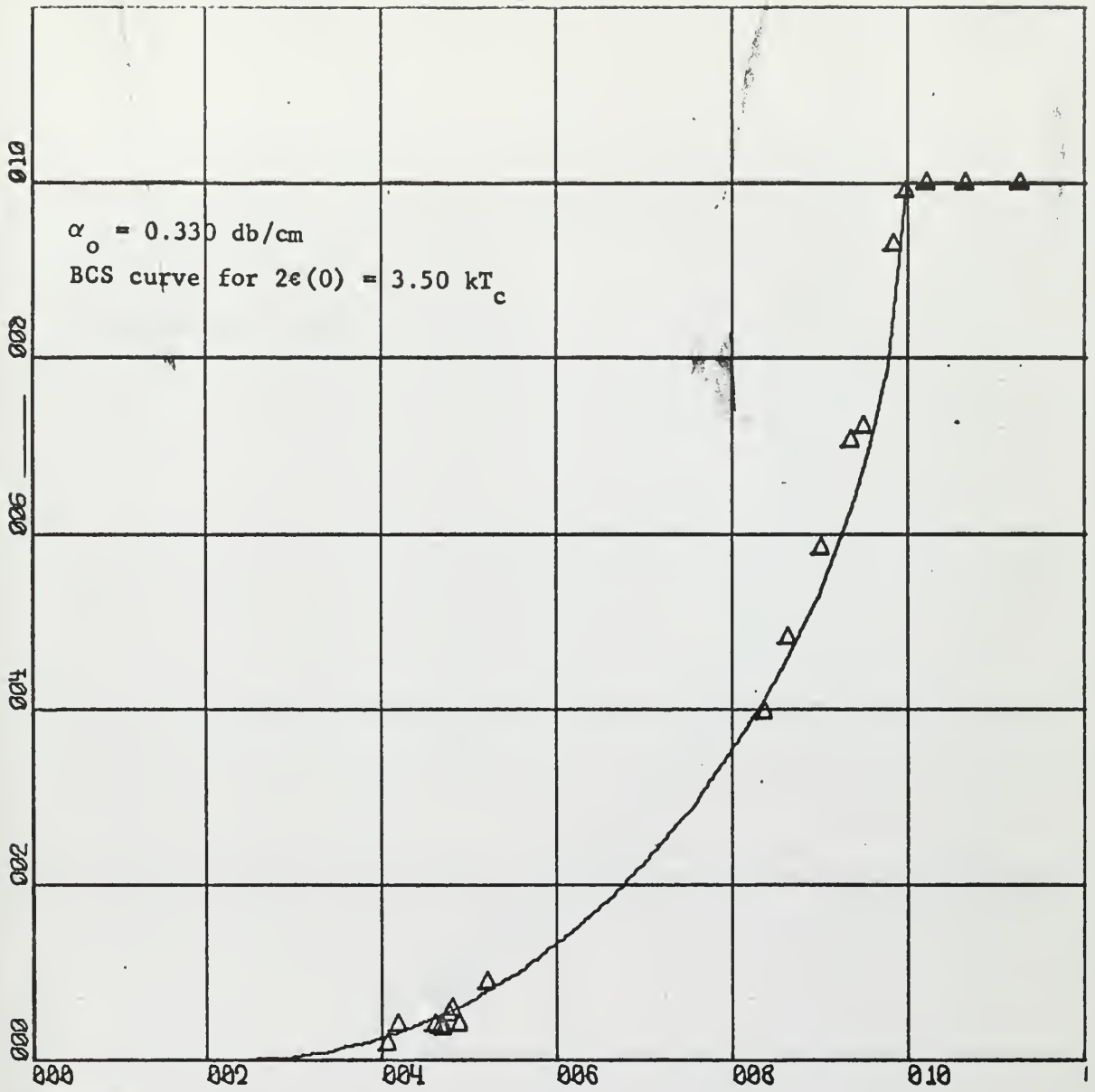
X-SCALE = $2.00E-01$ UNITS/INCH

Y-SCALE = $2.00E-01$ UNITS/INCH

GONCZ PROJECT 0321 13 NOV 64 30MCS
 REDUCED ATTENUATION VS REDUCED TEMPERATURE

Fig. 4

Fig. 4

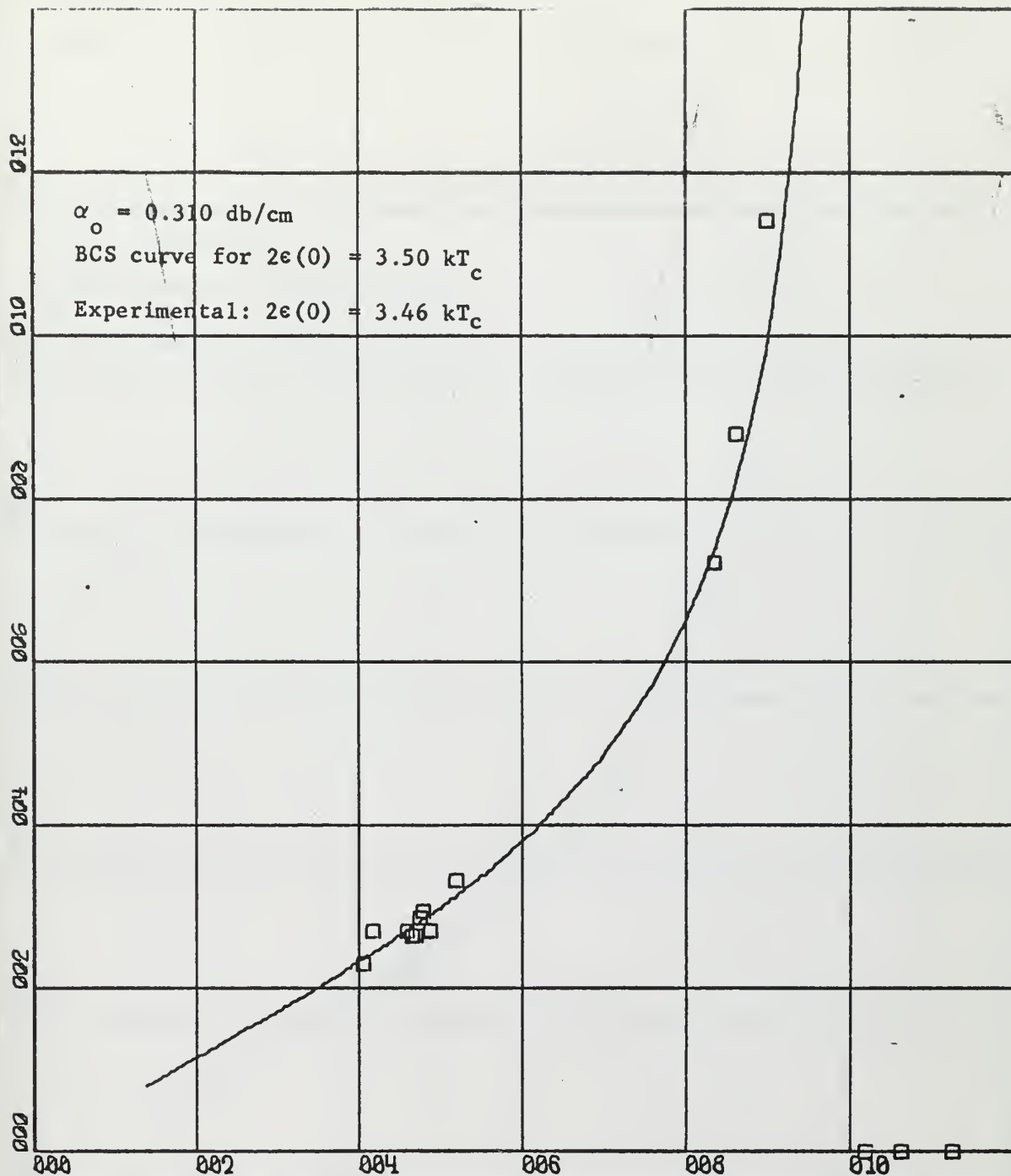


X-SCALE = 2.00E-01 UNITS/INCH.

Y-SCALE = 2.00E-01 UNITS/INCH.

GONCZ PROJECT 0321 13 NOV 64 30MCS
 REDUCED ATTENUATION VS REDUCED TEMPERATURE

Fig. 5

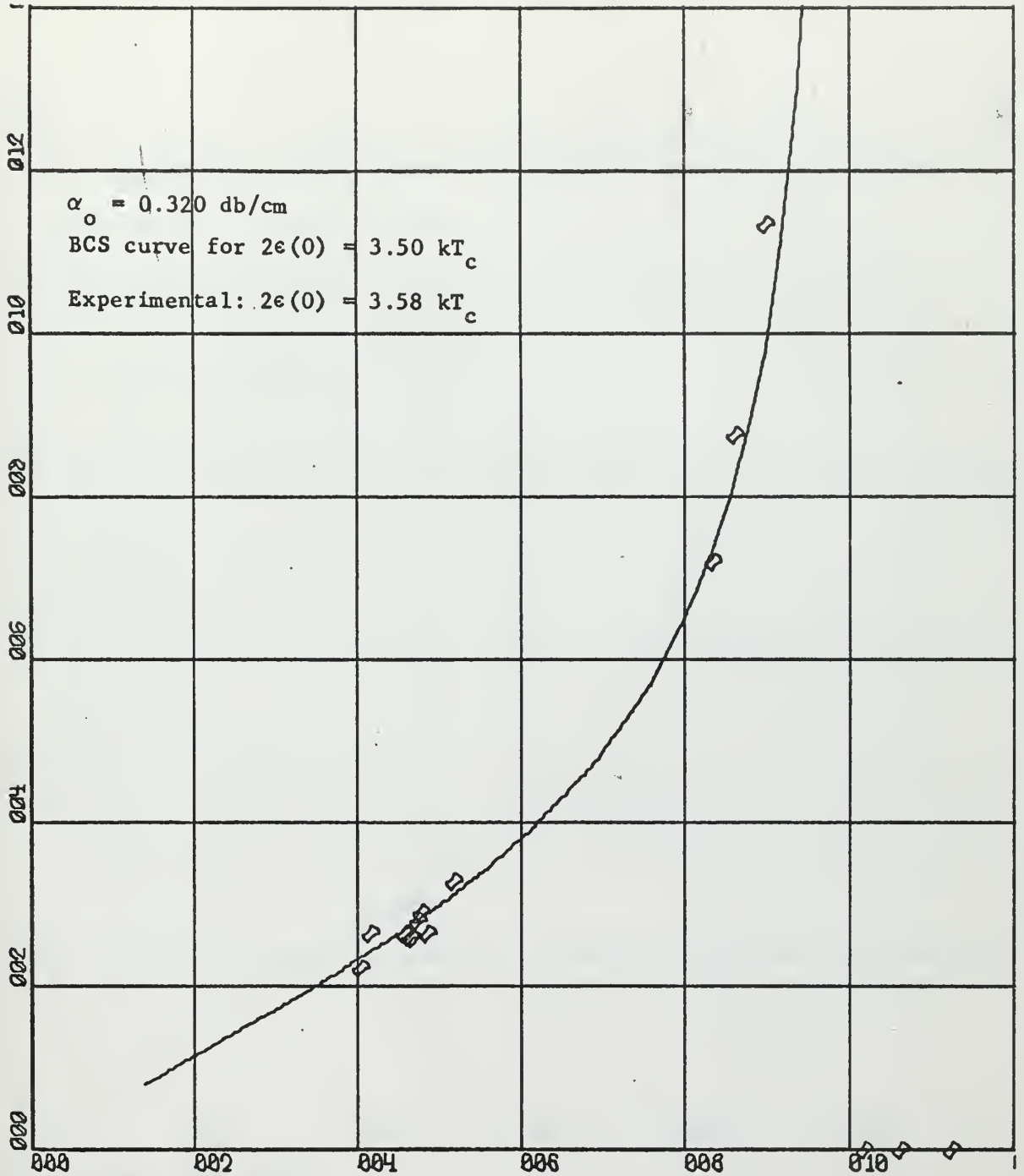


X-SCALE = 2.00E-01 UNITS/INCH

Y-SCALE = 2.00E-01 UNITS/INCH

GONCZ PROJECT 0321 13 NOV 64 30MCS
 $Y = 1 / (\text{LOG}(2 / \text{ALPHA} * - 1))$ VS REDUCED TEMPERATURE

Fig. 6

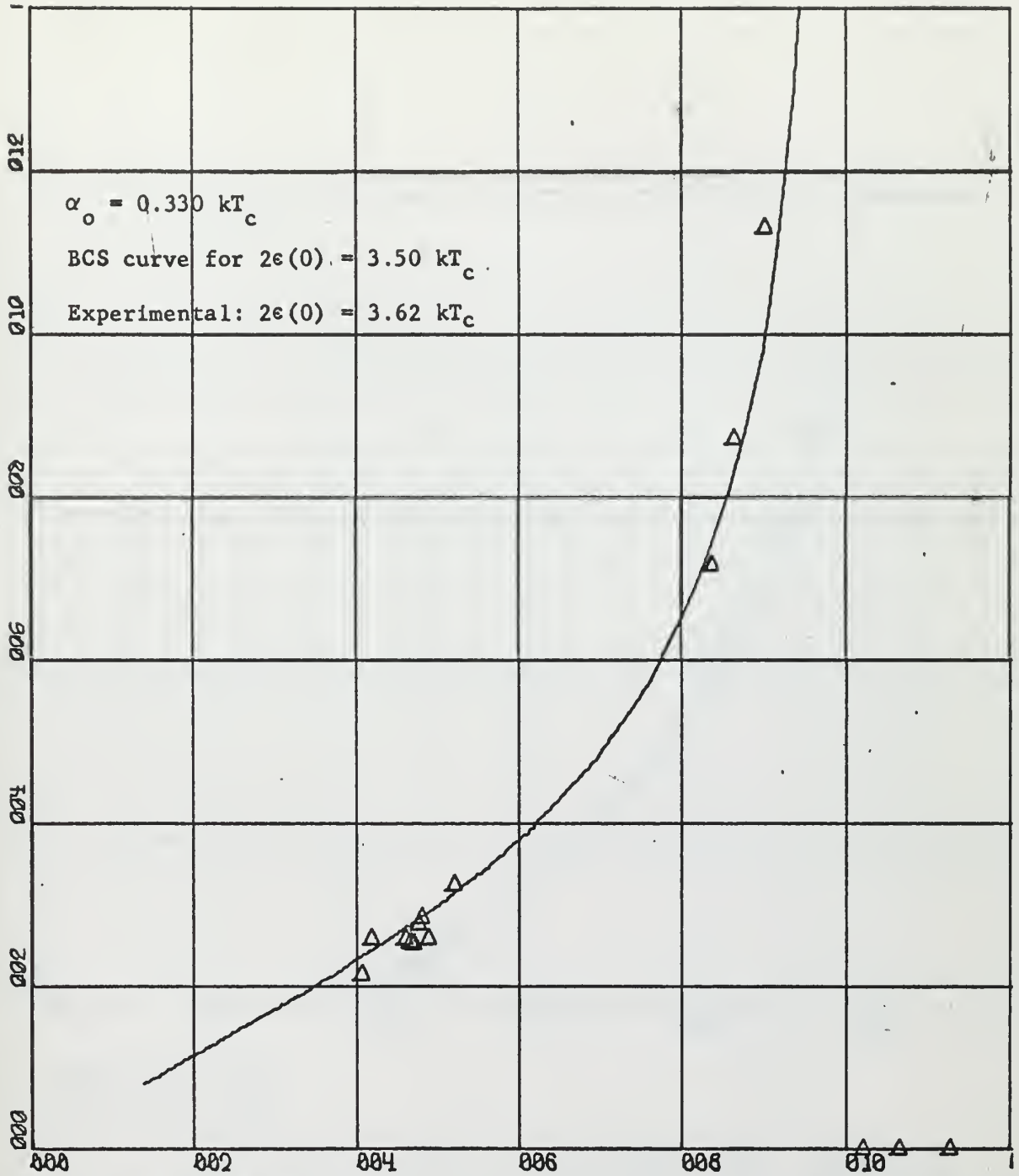


X-SCALE = 2.00E-01 UNITS/INCH

Y-SCALE = 2.00E-01 UNITS/INCH

GONCZ PROJECT 0321 13 NOV 64 30MCS
 $Y = 1 / (\log(2/\alpha - 1))$ VS REDUCED TEMPERATURE

Fig. 7

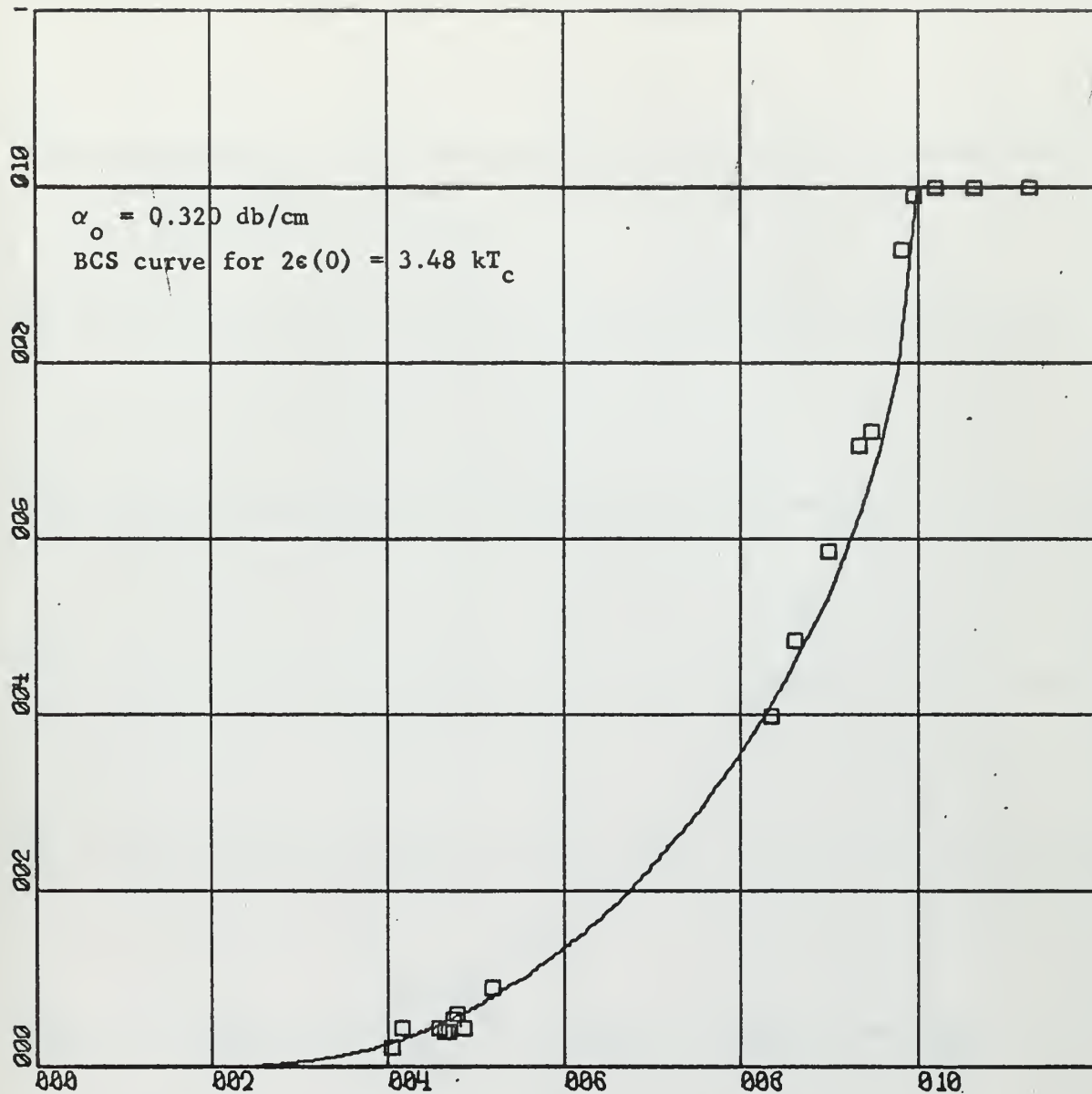


X-SCALE = 2.00E-01 UNITS/INCH

Y-SCALE = 2.00E-01 UNITS/INCH

GONCZ PROJECT 0321 13 NOV 64 30MCS
 Y = 1/(LOG(2/ALPHA - 1)) VS REDUCED TEMPERATURE

Fig. 8

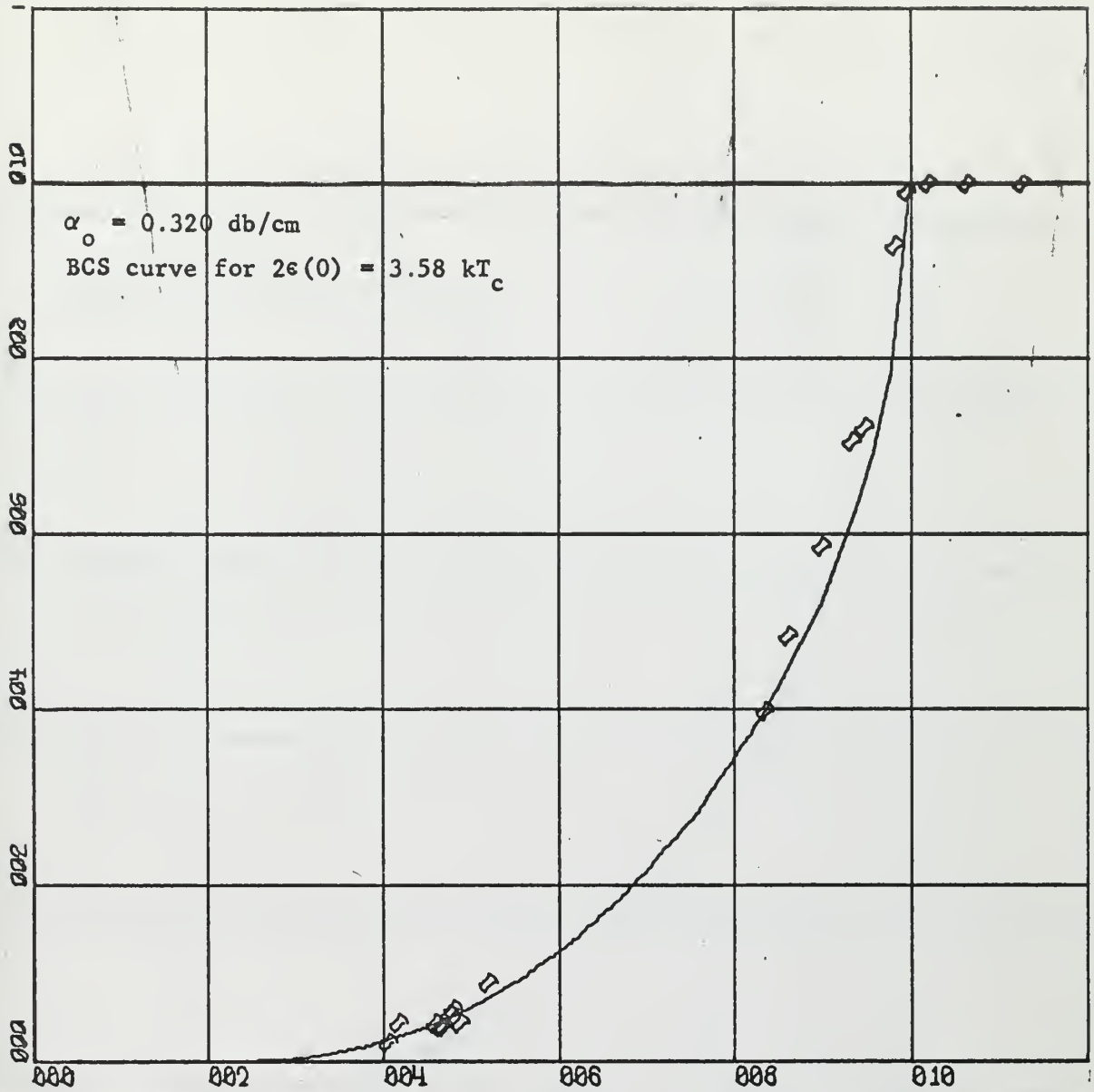


X-SCALE = 2.00E-01 UNITS/INCH

Y-SCALE = 2.00E-01 UNITS/INCH

GONCZ PROJECT 0321 13 NOV 64 30MCS
 REDUCED ATTENUATION VS REDUCED TEMPERATURE

Fig. 9

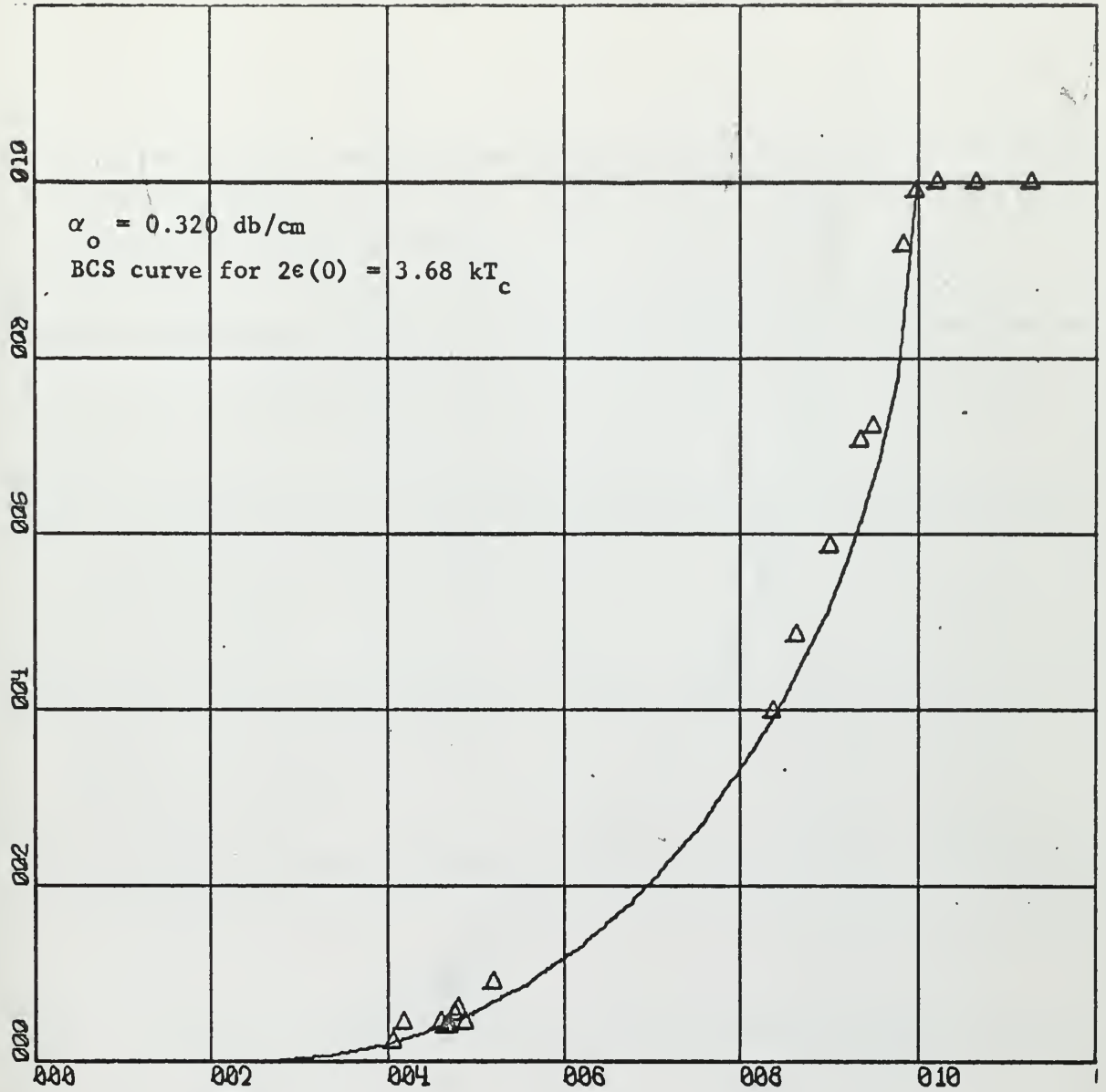


X-SCALE = 2.00E-01 UNITS/INCH

Y-SCALE = 2.00E-01 UNITS/INCH

GONCZ PROJECT 0321 13 NOV 64 30MCS
 REDUCED ATTENUATION VS REDUCED TEMPERATURE

Fig. 10

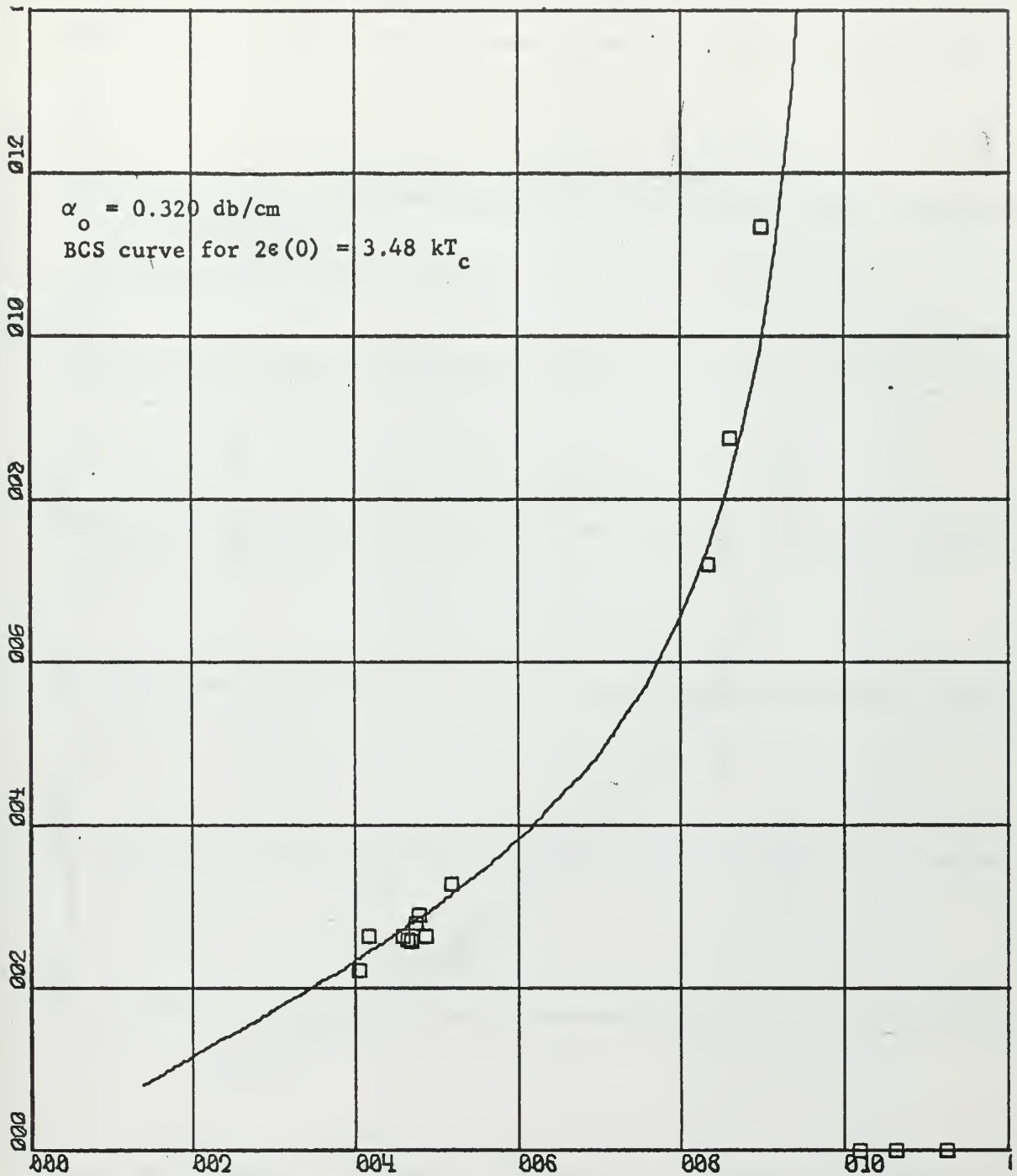


X-SCALE = 2.00E-01 UNITS/INCH.

Y-SCALE = 2.00E-01 UNITS/INCH.

GONCZ PROJECT 0321 13 NOV 64 30MCS
 REDUCED ATTENUATION VS REDUCED TEMPERATURE

Fig. 11

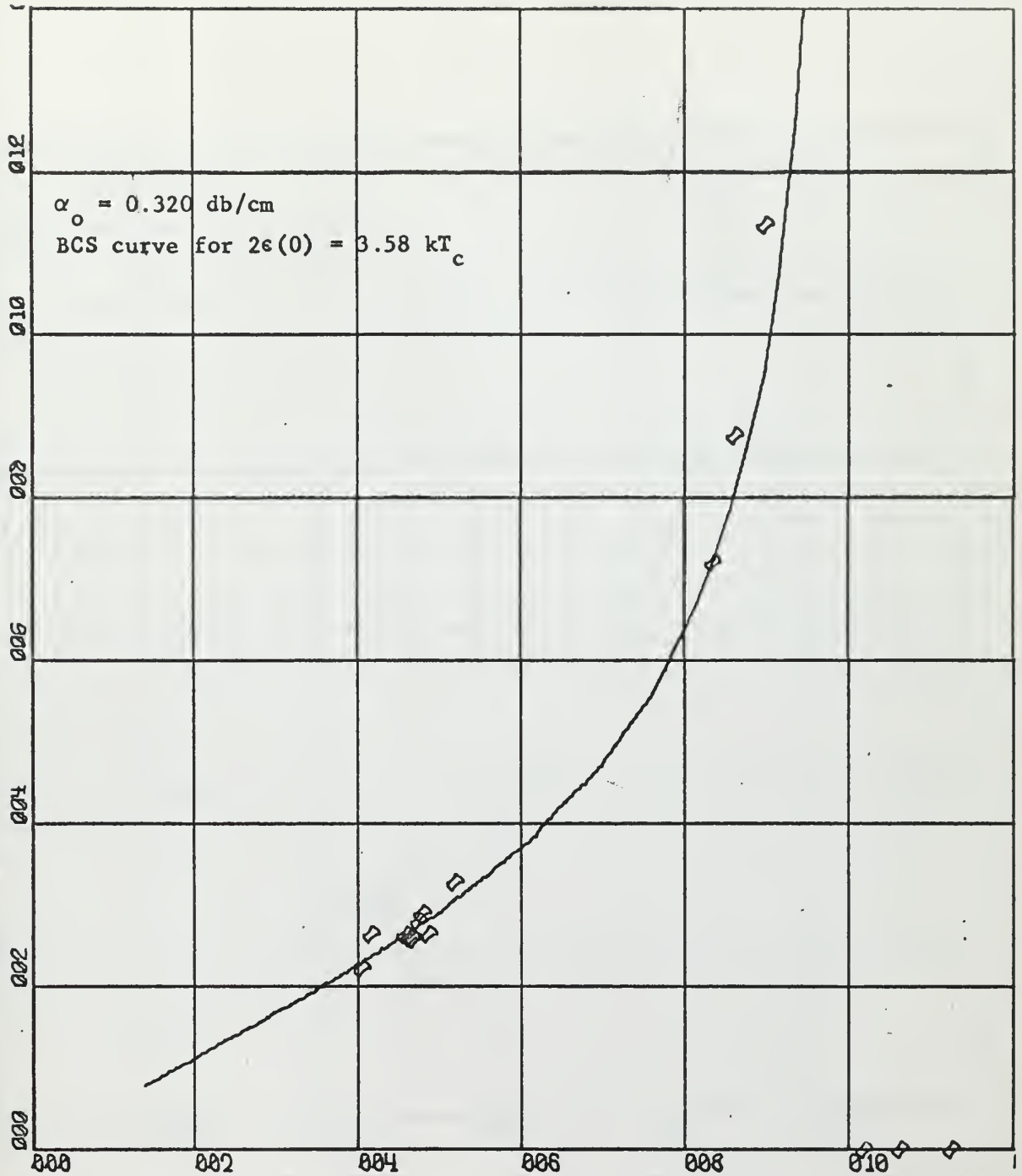


X-SCALE = 2.00E-01 UNITS/INCH.

Y-SCALE = 2.00E-01 UNITS/INCH.

GONCZ PROJECT 0321 13 NOV 64 30MCS
 $Y = 1 / (\text{LOG}(2 / \text{ALPHA}^* - 1))$ VS REDUCED TEMPERATURE

Fig. 12

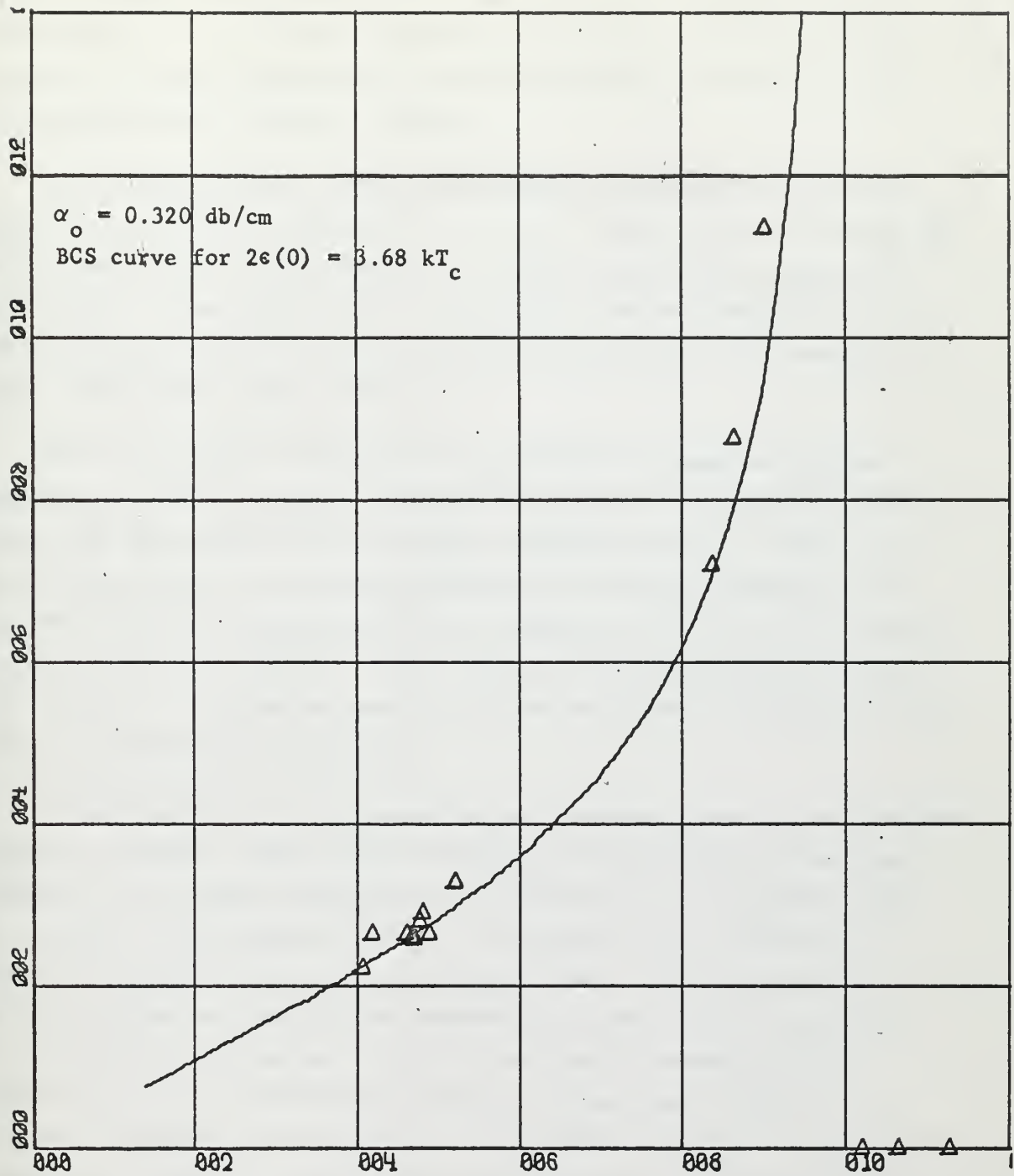


X-SCALE = 2.00E-01 UNITS/INCH

Y-SCALE = 2.00E-01 UNITS/INCH

GONCZ PROJECT 0321 13 NOV 64 30MCS
 $Y = 1 / (\text{LOG}(2 / \text{ALPHA}^* - 1))$ VS REDUCED TEMPERATURE

Fig. 13



X-SCALE = 2.00E-01 UNITS/INCH

Y-SCALE = 2.00E-01 UNITS/INCH

GONCZ PROJECT 0321 13 NOV 64 30MCS

$\ln(\ln(2/\alpha) - 1)$ VS REDUCED TEMPERATURE

Fig. 14

Figs. 6-8 depict the point plots of the function Y vs the reduced temperature, t , corresponding to the same values of residual attenuation. All these figures have the corresponding curve plots for the BCS expression for $2\epsilon(0) = 3.50 kT_c$.

The criterion used to find the residual attenuation and the zero degree gap was that on the plot of Y vs t the curve best fitting the experimental points should become a straight line passing through the origin for t less than 0.35. This follows from the expression for Y which becomes linear for $2/\alpha^*$ much greater than 1.00. The results of these analyses are given in Table I.

Once the residual attenuation was determined, computer program VARIGAP was used to show how changing the zero degree energy gap would change the BCS curves for the residual attenuation and Y . Figs. 9-11 show the BCS curve for reduced attenuation vs reduced temperature for a given residual attenuation and with changes of $0.10 kT_c$ in the energy gap determined from RESATT. Figs. 12-14 give the corresponding results for Y vs t . As can be seen the BCS curves do not shift much for the value of incremental change used.

It was found that the attenuation was constant above T_c and frequency dependent. Table I shows that attenuation increased with increasing frequency. The higher attenuation for 30 Mcs/sec in the normal state on 5 January 1965 compared to that of 13 November 1964 reflects the greater attenuation losses from the poorer bond. The value for the zero degree gap was gotten from computations based on semi-log plots. It is felt that this method is better than that of comparing echo heights since the latter method involves propagating through all the data any error made in measuring the echo height chosen as the basis for comparison. However, Table I shows that essentially the same results are obtained using either method. The difference in the methods is apparent in the different values of residual attenuation obtained. Taking

the value at the lowest temperature reached for comparing echo heights required that the residual attenuation be determined from this value rather than from an average of low temperature values as was done using semi-log plots.

TABLE 1

RESULTS OF RESATT COMPUTATIONS

Attenuation from Semi-log Plots

Run	Frequency Mcs/sec	Normal Attenuation α_n db/cm	Residual Attenuation α_o , db/cm	$\frac{2\zeta(0)}{KT_c}$	Results	
					α_o , db/cm	$\frac{2\zeta(0)}{KT_c}$
13 Nov 64	30	3.092	0.310	3.46	0.320	3.58
			0.320	3.58		
			0.330	3.62		
5 Jan 65	30	3.350	0.525	2.96	0.565	3.26
			0.565	3.26		
			0.605	3.49		
5 Jan 65	10	1.376	0.660	2.73	0.700	3.25
			0.700	3.25		
			0.740	3.63		

Attenuation from Comparison of Echo Heights

Run	Frequency Mcs/sec	Normal Attenuation α_n db/cm	Residual Attenuation α_o , db/cm	$\frac{2\zeta(0)}{KT_c}$	Results	
					α_o , db/cm	$\frac{2\zeta(0)}{KT_c}$
13 Nov 64	30	3.092	0.290	3.45	0.300	3.58
			0.300	3.58		
			0.310	3.65		
5 Jan 65	30	3.350	0.525	2.75	0.585	3.30
			0.565	2.99		
			0.605	3.57		
5 Jan 65	10	1.376	0.700	3.01	0.715	3.33
			0.715	3.33		
			0.730			

DISCUSSION OF RESULTS

The value obtained for the transition temperature, $T_c = 0.817^\circ\text{K}$, is lower than those of other investigators. However, those other experiments were determinations of the zero magnetic field transition temperature for zinc and show considerable variation. In heat capacity measurements, Phillips⁹ determined $T_c = 0.825^\circ\text{K}$. Geballe and Matthias¹⁰ in work on isotope effect measured $T_c = 0.855^\circ\text{K}$ and Cochran and Mapother¹¹ in critical field experiments found $T_c = 0.875^\circ\text{K}$. If a parabolic relationship between reduced magnetic field and reduced temperature is assumed

$$\frac{H}{H_c} = 1 - \left(\frac{T}{T_c} \right)^2,$$

where H_c is the critical magnetic field above which zinc will not become superconducting, then the transition temperature is reduced about five millidegrees for $H_c = 50$ gauss and $H = 0.5$ gauss. Thus $T_c = 0.817^\circ\text{K}$ agrees favorably with the lowest value quoted above.

Table II gives the results of several investigators who have measured the zero degree energy gap in zinc. There have been no ultrasonic attenuation measurements along the c-axis other than this one. The result of this work is higher than the value found by Biondi et al in a microwave absorption experiment in which there were "violent oscillations" in the data for $h\nu/kT_c$ less than 2.7. The measurement by Zemon and Boorse can only be taken as an average over all directions in the crystal. Bohm and Horowitz found the attenuation so great along the c-axis that they were unable to make any measurements. However, their measurement of the energy gap in two directions in the base plane and the measurements of the energy gap along the c-axis by Biondi and this work show anisotropies in the energy gap. These results also indicate that the gap along the c-axis is less than that predicted by the BCS theory and also is less than that for directions in the base plane.

TABLE II
ZERO DEGREE ENERGY GAP IN SUPERCONDUCTING ZINC

$2 \Delta(0)/kT_c$	Direction	T_c	Method	Investigator
3.8 ± 0.2	$[\bar{1}2\bar{1}0]$	0.85	Ultrasonic Attenuation 233 Mcs/sec	Bohm and Horowitz ¹³
3.4 ± 0.2	$[10\bar{1}0]$	0.85	Ultrasonic Attenuation 233 Mcs/sec	Bohm and Horowitz ¹²
3.00 ± 0.15	$[0001]$	0.838	Microwave Absorption 15-100 Gcs/sec	Biondi et al ¹³
3.01 ± 0.09	Polycrystalline Sample	0.825	Microwave Absorption 50-75 Gcs/sec	Zemon and Boorse ¹⁴
3.36 ± 0.13	$[0001]$	0.817	Ultrasonic Attenuation 10 & 30 Mcs/sec	Present Work

A more precise determination could be made if lower temperatures could be reached. The lowest temperature reached in this work was 0.320°K ; i.e., $0.38 t$. Thus to determine the energy gap, the experimental data had to be extrapolated some 40% on the reduced temperature scale.

The graphs of reduced attenuation vs reduced temperature can be fitted with a BCS curve quite well for low t . However, for t approaching 1.00, the experimental points lie above the BCS curve. Bohm and Horowitz don't report the comparison of their points with the BCS curve. However, investigators of other elements have found just the opposite; i.e., points for higher t lie below the BCS curve. For Niobium, Weber¹⁵ found the effect to be frequency dependent. With $T_c = 9.15^{\circ}\text{K}$, the BCS curve for the measured value of the energy gap, $3.63 kT_c$, fit the experimental points for 220 Mc/sec longitudinal wave along the [100] axis. However, for 30 Mc/sec the points lay below the BCS curve. He also found an isotropic result for the energy gap in the three crystallographic directions and suggested that any anisotropy in the gap may have been smeared out by impurity scattering. For thallium, $T_c = 2.38^{\circ}\text{K}$, Saunders and Lawson¹⁶ found that attenuation of longitudinal waves decreased more sharply below T_c than predicted by the BCS theory and that the anisotropy in the energy gap ranged from $(3.76 - 4.10)kT_c$.

These and similar results on other elements are in contrast to the findings of this work which should be investigated further. One basic assumption tacit in all these computations was that the residual attenuation was temperature independent. Though measurement above the transition temperature bore this out, the attenuation in the normal state for temperatures less than the zero magnetic field T_c should be measured. This might be done by placing the sample in a magnetic field to destroy the superconducting state.

Finally, measurements at higher frequencies should be carried out. Bobetic¹⁷ has carried out the calculations giving the ration of α_s/α_n

according to the BCS theory for an isotropic model at arbitrary frequencies and temperatures and predicted a discontinuity in attenuation at frequencies corresponding to the energy gap. This would require frequencies of the order 10^2 Gcs/sec.

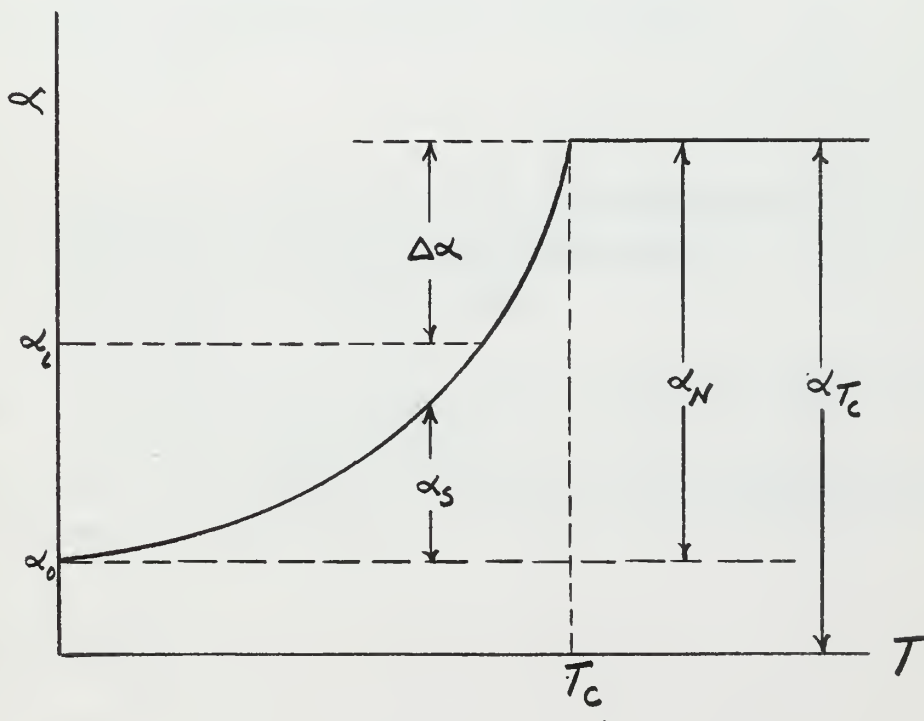
In this work attempts were made to make measurements at 50 and 70 Mcs/sec. However, so much power was needed to get an echo, that the sample heated excessively. Using a shorter sample would help solve this problem.

APPENDIX I
DATA ANALYSIS

Analysis begins by measuring the echo heights on each picture. This is most accurately done on an X-ray film reader to ± 0.01 mm. These heights are then plotted on semi-log graph paper vs echo number; one graph per picture. The slope of this graph is absolute attenuation per echo.

The basic problem in determining the absolute attenuation in the temperature range attained (4.2°K to approximately 0.320°K) is that the attenuation is so great from slightly below the superconducting transition temperature, T_c , to 4.2°K that one usually has only one echo. Below T_c , the attenuation drops rapidly and enough echoes appear to obtain the attenuation graphically.

A typical plot of absolute attenuation, α , vs temperature, T , is as follows:



where

α = absolute attenuation

α_o = residual attenuation

α_S = attenuation due to conduction electrons in the superconducting state

α_N = attenuation due to conduction electrons in the normal state

α_i = attenuation determined from raw data

T = Temperature - $^{\circ}$ K

T_c = Superconducting transition temperature

$\Delta\alpha$ = Change in attenuation between the superconducting and normal states

The slope of the semi-log plots are in echo^{-1} . The attenuation in db/cm is given as follows:

$$\text{Attenuation (db/cm)} = \frac{\text{Slope of Semi-log Plot} \times 8.6858}{2 \times \text{sample length in cm}}$$

We assume an exponential decay of echo heights.

$$A = A'e^{-\alpha \cdot n}$$

Let

A_i = amplitude of n^{th} echo in the superconducting state

A_N = amplitude of n^{th} echo in the normal state

A' = amplitude of the initial pulse

n = echo number

α_{T_c} = attenuation in the normal state from T_c to 4.2° K; a constant as verified experimentally

α_i = temperature dependent attenuation in the superconducting state

L = sample length in cm

Then

$$A_N = A'e^{-\alpha_{T_c} \cdot n}$$

$$A_i = A'e^{-\alpha_i \cdot n}$$

$$\text{Ln } A_N = \text{ln } A' - n \alpha_{T_c}$$

$$\text{Ln } A_i = \text{ln } A' - n \alpha_i$$

$$\text{ln} \left(\frac{A_i}{A_N} \right) = n (\alpha_{T_c} - \alpha_i) = -n \Delta\alpha$$

$$\text{or } \alpha_{T_c} \text{ (db/cm)} = \frac{8.6858}{2nL} \ln \left(\frac{A_i}{A_N} \right) + \alpha_i$$

To determine α_{T_c} from the single echo pictures above T_c , one computes α_{T_c} , with $n = 1$, for as many point by the above equation as one can from the semi-log plots. The best horizontal straight line fit to a plot of these points gives α_{T_c} . Then using the equation

$$\alpha_i \text{ (db/cm)} = \frac{8.6858}{2nL} \ln \left(\frac{A_N}{A_i} \right) + \alpha_N$$

gives the attenuation for the remaining points below T_c where there are not enough echoes to determine the attenuation from the semi-log plots.

Extrapolating the plot of α_i and α_{T_c} vs T to $T = 0$ will give an estimate of α_o . Where the curved part intersects the value for α_{T_c} determines T_c .

The quantity desired is the reduced attenuation $\alpha^* = \frac{\alpha_S}{\alpha_N}$, the ratio of attenuation due to conduction electrons alone in the superconducting and normal states vs $t = T/T_c$, the reduced temperature. Subtracting from α_i and α_{T_c} the quantity α_o which is attributed to impurity scattering, end losses, transducer losses, etc., gives

$$\alpha^* = \frac{\alpha_S}{\alpha_N} = \frac{\alpha_i - \alpha_o}{\alpha_{T_c} - \alpha_o}.$$

Subsequent calculations are very sensitive to the value α_o , which is not easily determined since one must extrapolate approximately 40% on the reduced temperature scale to $t = 0$ for zinc.

The BCS theory gives

$$\alpha^* = \frac{2}{e^{\epsilon(T)/kT} + 1}$$

for the variation of α^* for the longitudinal attenuation with T , where $\epsilon(T)$ is the temperature dependent energy gap between normal and superconducting electrons and k is the Boltzmann constant. What we want is

$\epsilon(0)$. The above expression can be inverted to give

$$Y = \frac{1}{\left[2/\alpha^* - 1\right]} = \left(\frac{kT_c}{\epsilon(t)}\right) t$$

This is the equation of a straight line passing through the origin when $2/\alpha^* \gg 1$. Hence, the slope at $t = 0$ for a plot of γ vs t gives the reciprocal of the zero degree superconducting energy gap in units of kT_c .

Data can also be analyzed by comparing the echo height of the same echo on each of the pictures. Then for a given n

$$\alpha_i (\text{db/cm}) = \frac{8.6858}{2nL} \ln \left(\frac{A_{no}}{A_{ni}} \right) + \alpha_o .$$

One must have some reference attenuation here denoted α_o to signify the attenuation at the lowest temperature reached. The attenuation can be most accurately determined at this point since the maximum number of echoes is present.

APPENDIX II
PROGRAM RESATT

The raw data; i.e., pictures, must be first analyzed in the manner outlined in Appendix I. Then the computer can be utilized to compute the reduced attenuation and the function Y, used to determine the zero degree superconducting energy gap, and plot these values separately as a function of the reduced temperature. Program RESATT, written in Fortran 60 language and compatible with the 1604 CDC computer, will accomplish these calculation. The primary purpose of this program is to determine the residual attenuation and to find the zero degree energy gap. The residual attenuation will be that value which when subtracted from the experimental values of attenuation will make Y, for t less than 0.4, plot as a straight line intercepting the origin.

For each set of data the program provides for the point plotting of computations based on three chosen values of the reduced attenuation, each set plotted on a separate graph. On each of these plots a theoretical curve based on the BCS expression, using a chosen zero degree energy gap, can be graphed. This is computed from values of $\epsilon(T)/\epsilon(0)$ vs t, the ratio of the temperature dependent energy gap to the zero degree energy gap versus reduced temperature as follows¹⁸:

$$\alpha^* = \frac{2}{\frac{C(I)EGAP}{2t} + 1}$$

Presently 44 values of C(I) are used. More can be computed from the reference.

The title, which must be changed for each set of data, identifies the experimenter, date on which data were taken, frequency, and computer project number. These are within the program itself. The program notes follow.

Code

TTR(I) - Reduced temperature, t, for theoretical BCS plot
 ATS(I) - Reduced attenuation, α^* , for theoretical BCS plot

TY(I) - $(\ln(2/\alpha^* - 1))^{-1}$, for theoretical BCS plot
 M - Number of data points for theoretical BCS plot, maximum number, 100
 EGAP - Zero degree energy gap, $2\epsilon(0)$, (no kT_c)
 C(I) - $\epsilon(TTR(I))/\epsilon(0)$
 N - Number of experimental values of T & α_i (up to 60)
 TC - Experimental value of Transition Temperature
 AN - Experimental value of $\alpha_n = \alpha_{T_c}$
 AZ(0) - Three experimental values of α_0
 T(I) - N experimental values of temperature
 A(I) - N experimental values of attenuation
 RT(I) - N values of reduced temperature

$\left. \begin{matrix} AS(1,I) \\ AS(2,I) \\ AS(3,I) \end{matrix} \right\}$ N values of $\alpha^* = \frac{\alpha - \alpha_0}{\alpha_n - \alpha_0}$ for $\left\{ \begin{matrix} AZ(0) - \text{small} \\ AZ(0) - \text{medium} \\ AZ(0) - \text{large} \end{matrix} \right.$

$\left. \begin{matrix} AY(1,I) \\ AY(2,I) \\ AY(3,I) \end{matrix} \right\}$ N values of $y = \frac{1}{\ln \left[\frac{2}{\alpha^*} - 1 \right]}$ for $\left\{ \begin{matrix} AZ(0) - \text{small} \\ AZ(0) - \text{medium} \\ AZ(0) - \text{large} \end{matrix} \right.$

Plots: Two sets of point plots

First: Three plots of α^* vs t,

Experimental Points AS(1,I) vs RT(I) for AZ(0) small - \square
 Experimental Points AS(2,I) vs RT(I) for AZ(0) medium - \diamond
 Experimental Points AS(3,I) vs RT(I) for AX(0) large - \triangle

Each will have the theoretical BCS curve ATS(I) vs TTR(I) plotted on the same graph.

Second: Three plots of Y vs t,

Experimental Points AY(1,I) vs RT(I) for AZ(0) small - \square
 Experimental Points AY(2,I) vs RT(I) for AZ(0) medium - \diamond
 Experimental Points AY(3,I) vs RT(I) for AZ(0) large - \triangle

Each of these will have the theoretical BCS curve TY(I) vs TTR(I) plotted on the same graph.



For each run a total of $3 + M + N$ cards are needed in the following order. The last digit of each input in each column in the stated order is to be in the 10, 20, 30, etc., column of the data card.

Number of cards	Input
1	M, EGAP
1 - M	Card No., TTR(I), C(I)
1	N, AN, TC
1 - N	Card No., T(I), A(I)
1	AZ(1), AZ(2), AZ(3)

Following is a complete print out of RESATT with the card deck composed for the data of 13 Nov 64. Card 000-197 comprise the program and cards 200-243 are the Mühlschlegel values. As outlined, the cards to be changed for a different set of data would be 57-61, 199, and 244-265.


```

000000
000010
000020
000030
000040
000050
000060
000070
000080
000090
000100
000110
000120
000130
000140
000150
000160
000170
000180
000190
000200
000210
000220
000230
000240
000250
000260
000270
000280
000290
000300
000310
000320
000330
000340

..JOB0321F,GONCZ
PROGRAM RESATT
DIMENSION X(900),Y(900),ITITLE(12),TTR(100),C(100),ATS(100),TY(100)
1),T(60),A(60),AS(3,30),AY(3,30),RT(30),AZ(3)
DO 1 I=1,900
X(I)=0.
1 Y(I)=0.
DO 2 I=1,12
2 ITITLE(I)=8H
DO 3 I=1,100
TTR(I)=0.
C(I)=0.
ATS(I)=0.
3 TY(I)=0.
DO 4 I=1,60
T(I)=0.
4 A(I)=0.
DO 5 J=1,30
RT(J)=0.
DO 5 I=1,3
AS(I,J)=0.
5 AY(I,J)=0.
DO 6 I=1,3
6 AZ(I)=0.
READ 50,M,EGAP
50 FORMAT (I10,F10.0)
DO 7 J=1,M
7 READ 9,(I,TTR(I),C(I))
READ 9,N,AN,TC
DO 8 J=1,N
8 READ 9,(I,T(I),A(I))
9 FORMAT(I10,2F10.0)
READ 10,AZ
10 FORMAT(3F10.0)
DO 11 I=1,M

```



```

IF(TTR(I))51,51,52
51 AT5(I)=0.
53 TY(I)=0.
GO TO 11
52 AT5(I)=2./((EXP(EGAP*C(I))/(2.*TTR(I)))+1.)
DUNK=2./AT5(I)-1.
IF(DUNK-1.)53,53,54
54 TY(I)=1./LOGF(DUNK)
11 CONTINUE
12 N=30
13 DO 16 J=1,N
RT(J)=T(J)/TC
DO 16 I=1,3
AS(I,J)=(A(J)-AZ(I))/(AN-AZ(I))
DUNK=2./AS(I,J)-1.
IF(DUNK-1.)14,14,15
14 AY(I,J)=0.
GO TO 16

```

```

15 AY(I,J)=1./LOGF(DUNK)
16 CONTINUE
LABEL=8H
ITITLE(1)=8H GO
ITITLE(2)=8HNCZ PRO
ITITLE(3)=8HJECT 032
ITITLE(4)=8H1 13 NOV
ITITLE(5)=8H 64 30M
ITITLE(6)=8HCS
ITITLE(7)=8H REDUC
ITITLE(8)=8HED ATTEN
ITITLE(9)=8HUATION V
ITITLE(10)=8HS REDUCE
ITITLE(11)=8HD TEMPER
ITITLE(12)=8HATURE
EXSCALE=0.2

```

```

000350
000360
000370
000380
000390
000400
000410
000420
000430
000440
000450
000460
000470
000480
000490
000500
000510
000520
000530
000540
000550
000560
000570
000580
000590
000600
000610
000620
000630
000640
000650
000660
000670
000680
000690

```



```

YSCALE=0.2
IXUP=0
IYRIGHT=0
MODEXAX=0
MODEYAX=0
IWIDE=8
IHIGH=8
IGRID=1
LAST=0
DO 20 I=1,3
NUMPTS=M
DO 17 J=1,M
X(J)=TTR(J)
17 Y(J)=ATS(J)
MODCURV=1
ITYPE=0
CALL DRAW(NUMPTS,X,Y,MODCURV,ITYPE,LABEL,ITITLE,EXSCALE,YSCALE,
1 IXUP,IYRIGHT,MODEXAX,MODEYAX,IWIDE,IHIGH,IGRID,LAST)
DO 18 J=1,M
X(J)=0.
18 Y(J)=0.
NUMPTS=N
DO 19 J=1,N
X(J)=RT(J)
19 Y(J)=AS(I,J)
MODCURV=3
ITYPE=I+2
CALL DRAW(NUMPTS,X,Y,MODCURV,ITYPE,LABEL,ITITLE,EXSCALE,YSCALE,
1 IXUP,IYRIGHT,MODEXAX,MODEYAX,IWIDE,IHIGH,IGRID,LAST)
DO 20 J=1,N
X(J)=0.
20 Y(J)=0.
ITITLE(7)=8H Y=1/(L
ITITLE(8)=8HOG(2/ALP
ITITLE(9)=8HHA*(-1))

```

```

000700
000710
000720
000730
000740
000750
000760
000770
000780
000790
000800
000810
000820
000830
000840
000850
000860
000870
000880
000890
000900
000910
000920
000930
000940
000950
000960
000970
000980
000990
001000
001010
001020
001030
001040

```



```

001050 ITITLE(10)=8HVS REDUC
001060 ITITLE(11)=8HED TEMPE
001070 ITITLE(12)=8HRATURE
001080 IHIGH=12
001090 DO 24 I=1,3
001100 NUMPTS=M-1
001110 DO 21 J=1,M
001120 X(J)=TTR(J)
001130 21 Y(J)=TY(J)
001140 MODCURV=1
001150 ITYPE=0
001160 CALL DRAW(NUMPTS,X,Y,MODCURV,ITYPE,LABEL,ITITLE,EXSCALE,YSCALE,
001170 1IXUP,IYRIGHT,MODEXAX,MODEYAX,IWIDE,IHIGH,IGRID,LAST)
001180 DO 22 J=1,M
001190 X(J)=0.
001200 22 Y(J)=0.
001210 NUMPTS=N
001220 DO 23 J=1,N
001230 X(J)=RT(J)
001240 23 Y(J)=AY(I,J)
001250 MODCURV=3
001260 ITYPE=I+2
001270 CALL DRAW(NUMPTS,X,Y,MODCURV,ITYPE,LABEL,ITITLE,EXSCALE,YSCALE,
001280 1IXUP,IYRIGHT,MODEXAX,MODEYAX,IWIDE,IHIGH,IGRID,LAST)
001290 DO 24 J=1,N
001300 X(J)=0.
001310 24 Y(J)=0.
001320 PRINT 27
001330 270FORMAT (88H1
001340 1DUCED TEMPERATURE///)
001350 PRINT 28,EGAP
001360 28 FORMAT (69H
001370 1LUES FOR E(0)=,F4.2,5H*K*TC)
001380 PRINT 29
001390 290FORMAT (58H
ALPHA * V S R E
THEORETICAL VA
REDU

```




11	0.34	0.9938	002100
12	0.36	0.9915	002110
13	0.38	0.9885	002120
14	0.40	0.9850	002130
15	0.42	0.9809	002140
16	0.44	0.9760	002150
17	0.46	0.9704	002160
18	0.48	0.9641	002170
19	0.50	0.9569	002180
20	0.52	0.9488	002190
21	0.54	0.9399	002200
22	0.56	0.9299	002210
23	0.58	0.9190	002220
24	0.60	0.9070	002230
25	0.62	0.8939	002240
26	0.64	0.8796	002250
27	0.66	0.8640	002260
28	0.68	0.8471	002270
29	0.70	0.8288	002280
30	0.72	0.8089	002290
31	0.74	0.7874	002300
32	0.76	0.7640	002310
33	0.78	0.7386	002320
34	0.80	0.7110	002330
35	0.82	0.6810	002340
36	0.84	0.6480	002350
37	0.86	0.6117	002360
38	0.88	0.5715	002370
39	0.90	0.5263	002380
40	0.92	0.4749	002390
41	0.94	0.4148	002400
42	0.96	0.3416	002410
43	0.98	0.2436	002420
44	1.00	0.0000	002430
20	3.092	0.817	002440

002450
002460
002470
002480
002490
002500
002510
002520
002530
002540
002550
002560
002570
002580
002590
002600
002610
002620
002630
002640
002650

0.574
0.444
0.491
0.474
0.434
0.436
0.444
0.445
0.383
1.427
1.664
1.945
2.280
2.325
2.894
3.065
3.092
3.092
3.092
3.092
0.330

0.422
0.396
0.390
0.386
0.381
0.378
0.373
0.339
0.330
0.683
0.703
0.734
0.763
0.773
0.802
0.813
0.833
0.868
0.919
1.011
0.320

1
2
3
4
5
6
7
8
9
10
11
12
13
14
15
16
17
18
19
20
0.310



APPENDIX III
PROGRAM VARIGAP

Once the best value of the residual attenuation and a determination of the zero degree energy gap has been made from RESATT, VARIGAP will compute and plot the theoretical BCS curves of reduced attenuation vs. reduced temperature and the function Y vs reduced temperature for three different zero degree energy gaps. On each of these will be the corresponding experimental points for one set of data and the chosen residual attenuation. To the extent that they differ from RESATT, the program notes for VARIGAP follow.

CODE

EGAP(I) - Three values of the zero degree energy gap (no kTc)

AS - One value of the residual attenuation

ATS(1,I)	} M theoretical values of reduced attenuation from the BCS expression	for	{	EGAP - small
ATS(2,I)				EGAP - medium
ATS(3,I)				EGAP - large

TY(1,I)	} M theoretical values of Y from the BCS expression	for	{	EGAP - small
TY(2,I)				EGAP - medium
TY(3,I)				EGAP - large

AS(J) - N experimental values of reduced attenuation

AY(J) - N experimental values of Y

PLOTS: Two sets of curve plots

First: Theoretical reduced attenuation vs reduced temperature

ATS(1,I) vs TTR(I) for EGAP - small - □
 ATS(2,I) vs TTR(I) for EGAP - medium - ◇
 ATS(3,I) vs TTR(I) for EGAP - large - △

Each of these will have point plotted on them the N experimental values of AS(J) vs T(J).

Second: Theoretical Function Y vs Reduced Temperature

TY(1,I) vs TTR(I) for EGAP small
 TY(2,I) vs TTR(I) for EGAP medium
 TY(3,I) vs TTR(I) for EGAP large

Each of these will have point plotted on them the N experimental values AY(J) vs T(J).

For each run a total of 3 + M + N cards are needed plus the correct title cards. The last digit of each input in each column in the stated order is to be in the 10, 20, 30, etc., column of the data card.

Number of Cards	Input
1	M, EGAP(low), EGAP(medium),EGAP(large)
1 - M	Card No., TTR(I), C(I)
1	N, AN, TC
1 - N	Card No., T(J), A(J)
1	AZ

Following is a complete print out of VARIGAP with the card deck composed for the data of 13 Nov 64. Cards 000 - 188 comprise the program. As outlined, the cards to be changed for a different set of data would be 57 - 61, 190, and 235 - 257.


```

000000
000010
000020
000030
000040
000050
000060
000070
000080
000090
000100
000110
000120
000130
000140
000150
000160
000170
000180
000190
000200
000210
000220
000230
000240
000250
000260
000270
000280
000290
000300
000310
000320
000330
000340
000350
000360

..JOB0321F,GONCZ
PROGRAM VARI GAP
DIMENSION X(900),Y(900),ITITLE(12),TTR(100),C(100),ATS(3,100),TY(3
1,100),T(60),A(60),AS(30),AY(30),RT(30),EGAP(3)
DO 1 I=1,900
X(I)=0.
1 Y(I)=0.
DO 2 I=1,12
2 ITITLE(I)=8H
DO 3 I=1,100
TTR(I)=0.
C(I)=0.
DO 3 J=1,3
ATS(J,I)=0.
3 TY(J,I)=0.
DO 4 I=1,60
T(I)=0.
4 A(I)=0.
DO 5 J=1,30
RT(J)=0.
AS(J)=0.
5 AY(J)=0.
DO 6 I=1,3
EGAP(I)=0.
6 EGAP(I)=0.
READ 50,M,EGAP
50 FORMAT (I10,3F10.0)
DO 7 J=1,M
7 READ 9,(I,TTR(I),C(I))
READ 9,N,AN,TC
DO 8 J=1,N
8 READ 9,(I,T(I),A(I))
9 FORMAT(I10,2F10.0)
READ 10,AZ
10 FORMAT (F10.0)
DO 11 J=1,3
DO 11 I=1,M
IF(TTR(I))51,51,52

```

1881

1882

1883

1884

1885

1886

1887

1888

1889

1890

1891

1892

1893

1894

1895

1896

1897

1898

1899

1900

1901

1902

1903

1904

1905

```

000370
000380
000390
000400
000410
000420
000430
000440
000450
000460
000470
000480
000490
000500
000510
000520
000530
000540
000550
000560
000570
000580
000590
000600
000610
000620
000630
000640
000650
000660
000670
000680
000690
000700
000710
000720
000730

51 ATS(J,I)=0.
53 TY(J,I)=0.
   GO TO 11
52 ATS(J,I)=2./(EXPF(EGAP(J)*C(I))/(2.*TTR(I)))+1.)
   DUNK=2./ATS(J,I)-1.
   IF(DUNK-1.)53,53,54
54 TY(J,I)=1./LOGF(DUNK)
11 CONTINUE
   IF(N-30)13,13,12
12 N=30
13 DO 16 J=1,N
   RT(J)=T(J)/TC
   AS(J)=(A(J)-AZ)/(AN-AZ)
   DUNK=2./AS(J)-1.
   IF(DUNK-1.)14,14,15
14 AY(J)=0.
   GO TO 16
15 AY(J)=1./LOGF(DUNK)
16 CONTINUE
   LABEL=8H
   ITITLE(1)=8H      GO
   ITITLE(2)=8HNCZ  PRO
   ITITLE(3)=8HJECT 032
   ITITLE(4)=8H1 13 NOV
   ITITLE(5)=8H 64 30M
   ITITLE(6)=8HCS
   ITITLE(7)=8H      REDUC
   ITITLE(8)=8HED  ATTEN
   ITITLE(9)=8HUATION V
   ITITLE(10)=8HS  REDUCE
   ITITLE(11)=8HD  TEMPER
   ITITLE(12)=8HATURE
   EXSCALE=0.2
   YSCALE=0.2
   IXUP=0
   IYRIGHT=0
   MODEXAX=0

```



```

MODEYAX=0
IWIDTH=8
IHIGH=8
IGRID=1
LAST=0
DO 20 I=1,3
NUMPTS=M
DO 17 J=1,M
X(J)=TTR(J)
17 Y(J)=ATS(I,J)
MODCURV=1
ITYPE=0
CALL DRAW(NUMPTS,X,Y,MODCURV,ITYPE,LABEL,ITITLE,EXSCALE,YSCALE,
1 IXUP,IYRIGHT,MODEXAX,MODEYAX,IWIDE,IHIGH,IGRID,LAST)
DO 18 J=1,M
X(J)=0.
18 Y(J)=0.
NUMPTS=N
DO 19 J=1,N
X(J)=RT(J)
19 Y(J)=AS(J)
MODCURV=3
ITYPE=I+2
CALL DRAW(NUMPTS,X,Y,MODCURV,ITYPE,LABEL,ITITLE,EXSCALE,YSCALE,
1 IXUP,IYRIGHT,MODEXAX,MODEYAX,IWIDE,IHIGH,IGRID,LAST)
DO 20 J=1,N
X(J)=0.
20 Y(J)=0.
ITITLE(7)=8H Y=1/(L
ITITLE(8)=8HOG(2/ALP
ITITLE(9)=8HHA*-1))
ITITLE(10)=8HVS REDUC
ITITLE(11)=8HED TEMPE
ITITLE(12)=8HRATURE
IHIGH=12
DO 24 I=1,3
NUMPTS=M-1
DO 21 J=1,M

```

000740

000750

000760

000770

000780

000790

000800

000810

000820

000830

000840

000850

000860

000870

000880

000890

000900

000910

000920

000930

000940

000950

000960

000970

000980

000990

001000

001010

001020

001030

001040

001050

001060

001070

001080

001090

001100

001110


```

X(J)=TTR(J)
21 Y(J)=TY(I,J)
MODCURV=1
ITYPE=0
CALL DRAW(NUMPTS,X,Y,MODCURV,ITYPE,LABEL,ITITLE,EXSCALE,YSCALE,
IXUP,IYRIGHT,MODEXAX,MODEYAX,IWIDE,IHIGH,IGRID,LAST)
DO 22 J=1,M
X(J)=0.
22 Y(J)=0.
NUMPTS=N
DO 23 J=1,N
X(J)=RT(J)
23 Y(J)=AY(J)
MODCURV=3
ITYPE=I+2
CALL DRAW(NUMPTS,X,Y,MODCURV,ITYPE,LABEL,ITITLE,EXSCALE,YSCALE,
IXUP,IYRIGHT,MODEXAX,MODEYAX,IWIDE,IHIGH,IGRID,LAST)
DO 24 J=1,N
X(J)=0.
24 Y(J)=0.
PRINT 27
270FORMAT (88H1
IDUCED TEMPERATURE///)
PRINT 28
28 FORMAT (71H
ENTIAL VALUES FOR)
PRINT 29,AN,TC,AZ
29 FORMAT (40H
1 =,F8.5,11H AND AZ =,F8.5///)
PRINT 30
30 FORMAT (72H
REDUCED)
PRINT 31
31 FORMAT (86H
TEMPERATURE ALPHA*///)
PRINT 32,(T(I),A(I),RT(I),AS(I),I=1,N)
ALPHA * V S R E
EXPERIM
AN =,F8.5,9H , TC
TEMPERATURE ALPH

```

```

001120
001130
001140
001150
001160
001170
001180
001190
001200
001210
001220
001230
001240
001250
001260
001270
001280
001290
001300
001310
001320
001330
001340
001350
001360
001370
001380
001390
001400
001410
001420
001430
001440
001450
001460
001470

```



```

32 FORMAT ((F42.5,F12.5,F16.5,F14.6)///)
   PRINT 33
33 FORMAT (68H
   METICAL VALUES//)
   PRINT 34
34 FORMAT (43H
   PRINT 35
35 FORMAT (72H
   ALPHA*)
   PRINT 36
36 FORMAT (87H
   -----)
   PRINT 37
37 FORMAT (85H
   E

```

```

001480
001490
001500
001510
001520
001530
001540
001550
001560
001570
001580
001590
001600
001610

```

```

THEOR
REDUCED)
TEMPERATURE
-----
E

```

```

1GAP=
PRINT 38,EGAP
38 FORMAT (F59.3,2F13.3//)
39 FORMAT (F43.6,F17.6,2F13.6)
40 FORMAT (83H1
   I E D T E M P E R A T U R E///)
   PRINT 28
   PRINT 29,AN,TC,AZ
   PRINT 30
   PRINT 41
41 FORMAT (84H
   1A
   TEMPERATURE
   PRINT 32,(T(I),A(I),RT(I),AY(I),I=1,N)
   PRINT 33
   PRINT 34
   PRINT 42
42 FORMAT (70H
   TY)
   PRINT 36
   PRINT 37
   PRINT 38,EGAP

```

```

001620
001630
001640
001650
001660
001670
001680
001690
001700
001710
001720
001730
001740
001750
001760
001770
001780
001790
001800
001810
001820
001830
001840

```

```

Y V S R E D U C
TEMPERATURE
ALPH
TEMPERATURE
TEMPERATURE

```



PRINT 39,(TTR(I),TY(1,I),TY(2,I),TY(3,I),I=1,M)

STOP
END
END

44
1
2
3
4
5
6
7
8
9
10
11
12
13
14
15
16
17
18
19
20
21
22
23
24
25
26
27
28
29
30

3.48
0.14
0.16
0.18
0.20
0.22
0.24
0.26
0.28
0.30
0.32
0.34
0.36
0.38
0.40
0.42
0.44
0.46
0.48
0.50
0.52
0.54
0.56
0.58
0.60
0.62
0.64
0.66
0.68
0.70
0.72

3.58
1.0000
1.0000
1.0000
0.9999
0.9997
0.9994
0.9989
0.9982
0.9971
0.9957
0.9938
0.9915
0.9885
0.9850
0.9809
0.9760
0.9704
0.9641
0.9569
0.9488
0.9399
0.9299
0.9190
0.9070
0.8939
0.8796
0.8640
0.8471
0.8288
0.8089

3.68

001850
001860
001870
001880
001890
001900
001910
001920
001930
001940
001950
001960
001970
001980
001990
002000
002010
002020
002030
002040
002050
002060
002070
002080
002090
002100
002110
002120
002130
002140
002150
002160
002170
002180
002190
002200



002210
002220
002230
002240
002250
002260
002270
002280
002290
002300
002310
002320
002330
002340
002350
002360
002370
002380
002390
002400
002410
002420
002430
002440
002450
002460
002470
002480
002490
002500
002510
002520
002530
002540
002550
002560

0.7874
0.7640
0.7386
0.7110
0.6810
0.6480
0.6117
0.5715
0.5263
0.4749
0.4148
0.3416
0.2436
0.0000
0.817
0.574
0.444
0.491
0.474
0.434
0.436
0.444
0.445
0.383
1.427
1.664
1.945
2.280
2.325
2.894
3.065
3.092
3.092
3.092
3.092

0.74
0.76
0.78
0.80
0.82
0.84
0.86
0.88
0.90
0.92
0.94
0.96
0.98
1.00
3.092
0.422
0.396
0.390
0.386
0.381
0.378
0.373
0.339
0.330
0.683
0.703
0.734
0.763
0.773
0.802
0.813
0.833
0.868
0.919
1.011

31
32
33
34
35
36
37
38
39
40
41
42
43
44
20
1
2
3
4
5
6
7
8
9
10
11
12
13
14
15
16
17
18
19
20
0.320

APPENDIX IV
PROGRAM ZEROGAP

This program provides for a least square fit of experimental points to the BCS function

$$\frac{\alpha_s}{\alpha_N} = \frac{2}{\frac{\epsilon(T)}{e^{kT} + 1}}$$

by minimizing the square of the vertical distances from the curve to the experimental points. This is done using two parameters; the residual attenuation and the zero degree energy gap. The output of the program is the value of these two parameters. Since in the BCS expression α_s and α_N involve only the attenuation due to electron-phonon interaction, all other causes of attenuation must be subtracted out.

Thus,

$$\frac{\alpha' - \alpha_o}{\alpha_N - \alpha_o} = \frac{2}{\frac{\epsilon(T)}{e^{kT} + 1}}$$

or

$$\alpha' = \alpha_o + (\alpha_N - \alpha_o) \frac{2}{\frac{\epsilon(T)}{e^{kT} + 1}}$$

where α' and α_N would be on a BCS curve shifted an amount α_o due to residual attenuation.

What is desired is to minimize the residue

$$R = \sum_{i=1}^N (\alpha - \alpha')^2$$

where α is an experimental measurement of attenuation and N is the number of experimental points.

Let the following quantities be defined which will be used in the program.

α - A(I) - Experimental measurement of attenuation

t - RT(I) - The reduced temperature corresponding to the temperature T(I) at which A(I) was measured.



α_0 - AZ - Residual attenuation - one of two parameters to be determined
 $C(I)$ -US(I) - The Mühlischlegel values of $\epsilon(T)/\epsilon(0)$ vs t .

By use of an interpolating program, the values of $C(I)$ were obtained from the Mühlischlegel values for $0.191 \leq t \leq 1.000$ in increments of 0.001 and incorporated in the program. In the printout of the program following they are cards 200 - 910, where for example, 200 means $t=0.200$ and the number in the 10th column is $C(I)$ for the t .
 $C(I)/t$ - UC(I)

The equation for α' can then be written

$$\alpha' = \alpha_0 + (\alpha_N - \alpha_0) \frac{2}{\frac{C(I) \cdot 2 \epsilon(0)}{e^{2t}} + 1}$$

$$\text{Now let FER}(I) = \frac{1}{\frac{C(I) \cdot 2 \epsilon(0)}{e^{2t}} + 1} = \frac{1}{\text{EXP} \left[\frac{UC(I) \cdot \text{EGAP}}{2} \right] + 1}$$

where EGAP is the zero degree energy gap = $2 \epsilon(0)$ - the other parameter to be determined. Then the residue becomes

$$R = \sum_{i=1}^N \left[A(I) - AZ - (AN - AZ) 2\text{FER}(I) \right]^2.$$

From this an explicit expression for AZ can be gotten from the condition

$$\frac{\partial R}{\partial AZ} = 0.$$

Carrying out the steps gives

$$AZ = \frac{\sum_{i=1}^N \left[(2AN\text{FER}(I) - A(I)) \right] \left[2\text{FER}(I) - 1 \right]}{\sum_{i=1}^N \left[2\text{FER}(I) - 1 \right] \left[2\text{FER}(I) - 1 \right]}$$

in which terms cannot be canceled since they are under the summation signs. In this expression only FER depends on EGAP.

The other condition for minimizing the residue is $\frac{\partial R}{\partial EGAP} = 0$.

Carrying out the steps gives

$$\frac{\partial R}{\partial EGAP} = 2 \sum_{i=1}^N \left[A(I) - AZ - 2(AN - AZ)FER(I) \right] \\ \times \left[2(AZ - AN) - \frac{UC}{2} FER(FER - 1) \right]$$

So what is needed is to minimize $\sum \left[(2ANFER(I) - A(I)) - AZ(2FER - 1) \right] UC \\ \times \left[FER(FER - 1) \right] \left[AN - AZ \right]$

subject to the above value of AZ. The remainder of the program notes are the following:

$$ONE(I) = 2FER(I) - 1 \\ TWO(I) = 2ANFER(I) - A(I)$$

The inputs needed are the best guess of EGAP; AN, the experimental determination of the attenuation in the normal state; TC, the transition temperature; and the N data points of A(I) vs T(I).

One card contains N, AN, TC, and EGAP, the last digit of each is in column 10, 20, 30 and 40 respectively. Next follow the N data cards of A(I) vs T(I); one card for each set with the last digit of the card number in column 10, that of T(I) in 20, and that of A(I) in 30. A print out of the program follows at the end of the appendix. The input cards follow the blank card which must be added to the end of the program cards.

Table III gives the results of program Zerogap and compares them to those of program Resatt. Figs. 15-26 give the plots of the BCS curve, using the values of residual attenuation and the energy gap determined from Zerogap and the point plots of the corresponding experimental data.

It is evident that the program does what it is designed to do. However, the values of residual attenuation are markedly different in the 30 mcs/sec data from that obtained by extrapolation of the curve of attenuation vs temperature. For the 30 mcs/sec, 5 Jan 65, semi-log data the value obtained is unrealistic in that it is greater than most of the data points. Only the attainment of lower values of reduced temperature,

t, can resolve the question as to whether or not the value of residual attenuation obtained from Zerogap is realistic.

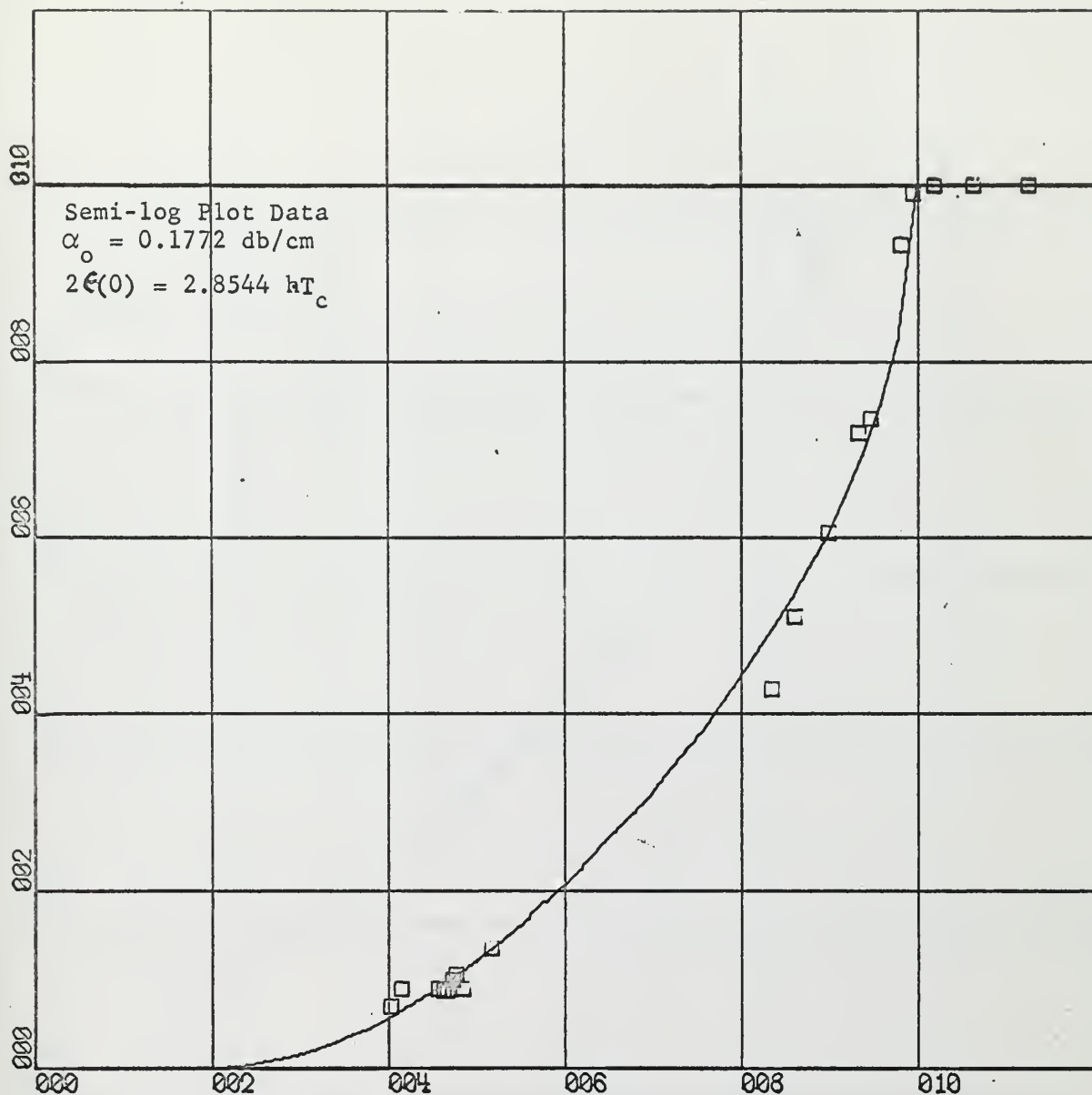
The program seems to work best when there are data points over the whole range of t; e.g., 30 Nov 64 and 5 Jan 65, 10 mcs/sec data. Also, when the points are not too scattered as in the 30 Nov 64 data, the results are reasonable. The values of $(2.85 \text{ and } 2.82)kT_c$ obtained for the energy gap for these data are reasonable bearing in mind the previous observation that for higher t the experimental points lie above the $3.50 kT_c$ BCS curve. As one can see the lower the value of the energy gap, the higher the BCS curve.

This program can be of use in interpreting data if one realizes that the analysis depends completely on the BCS theory and the simplifying assumptions used in obtaining the expression for the reduced attenuation and masks the possibility of other phenomenon taking place.

TABLE III

COMPARISON OF ZEROGAP AND RESATT RESULTS

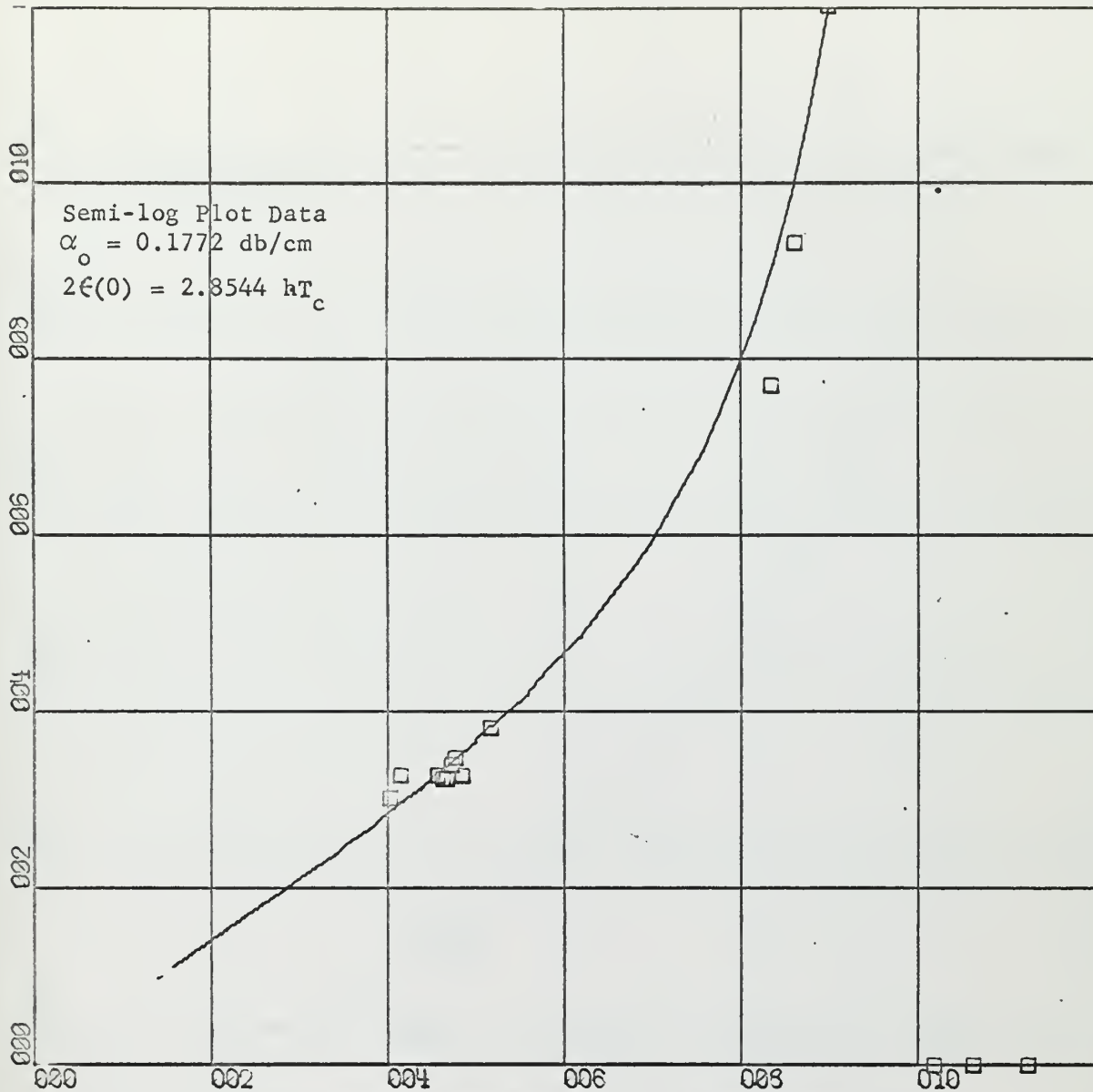
RUN	FREQUENCY Mcs/sec	TYPE	ZEROGAP		RESATT	
			RESIDUAL ATTENUATION db/cm	ENERGY GAP $2\epsilon(0)/kT_c$	RESIDUAL ATTENUATION db/cm	ENERGY GAP $2\epsilon(0)/kT_c$
13 Nov 64	30	Semi-log	0.1772	2.8544	0.320	3.58
13 Nov 64	30	Echo Heights	0.1507	2.8171	0.300	3.58
5 Jan 65	30	Semi-log	0.8755	7.2968	0.565	3.26
5 Jan 65	30	Echo Heights	0.4387	2.5304	0.585	3.30
5 Jan 65	10	Semi-log	0.7166	3.5941	0.700	3.25
5 Jan 65	10	Echo Heights	0.6097	2.1181	0.715	3.33



X-SCALE = 2.00E-01 UNITS/INCH.
 Y-SCALE = 2.00E-01 UNITS/INCH.

GONCZ PROJECT 0321 13 NOV 64 30MCS
 REDUCED ATTENUATION VS REDUCED TEMPERATURE

Fig. 15

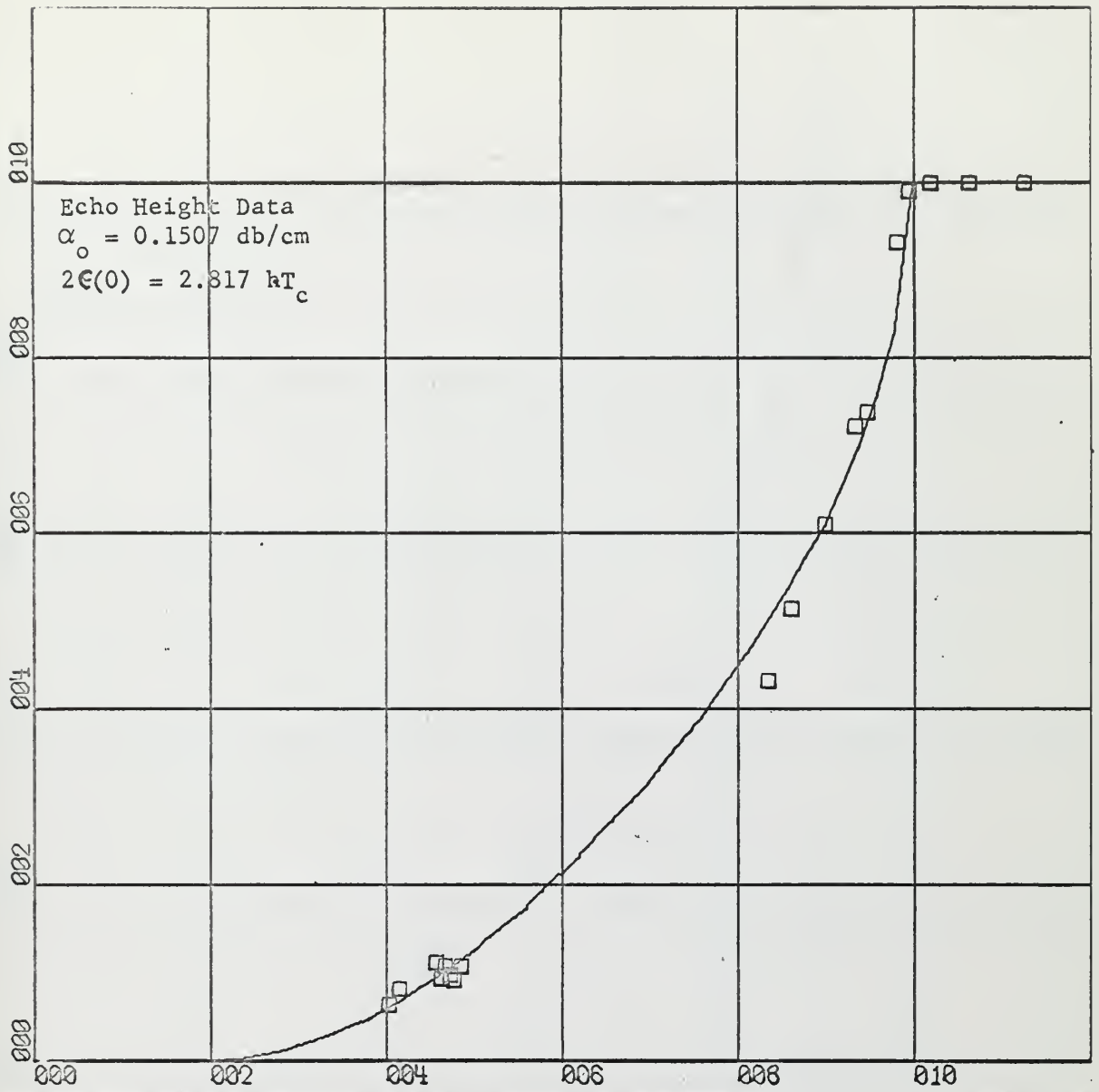


Y-SCALE = 2.00E-01 UNITS/INCH.

Y-SCALE = 2.00E-01 UNITS/INCH.

GONCZ PROJECT 0321 13 NOV 64 30MCS
 $\gamma = 1/(\text{LOG}(2/\text{ALPHA}^* - 1))$ VS REDUCED TEMPERATURE

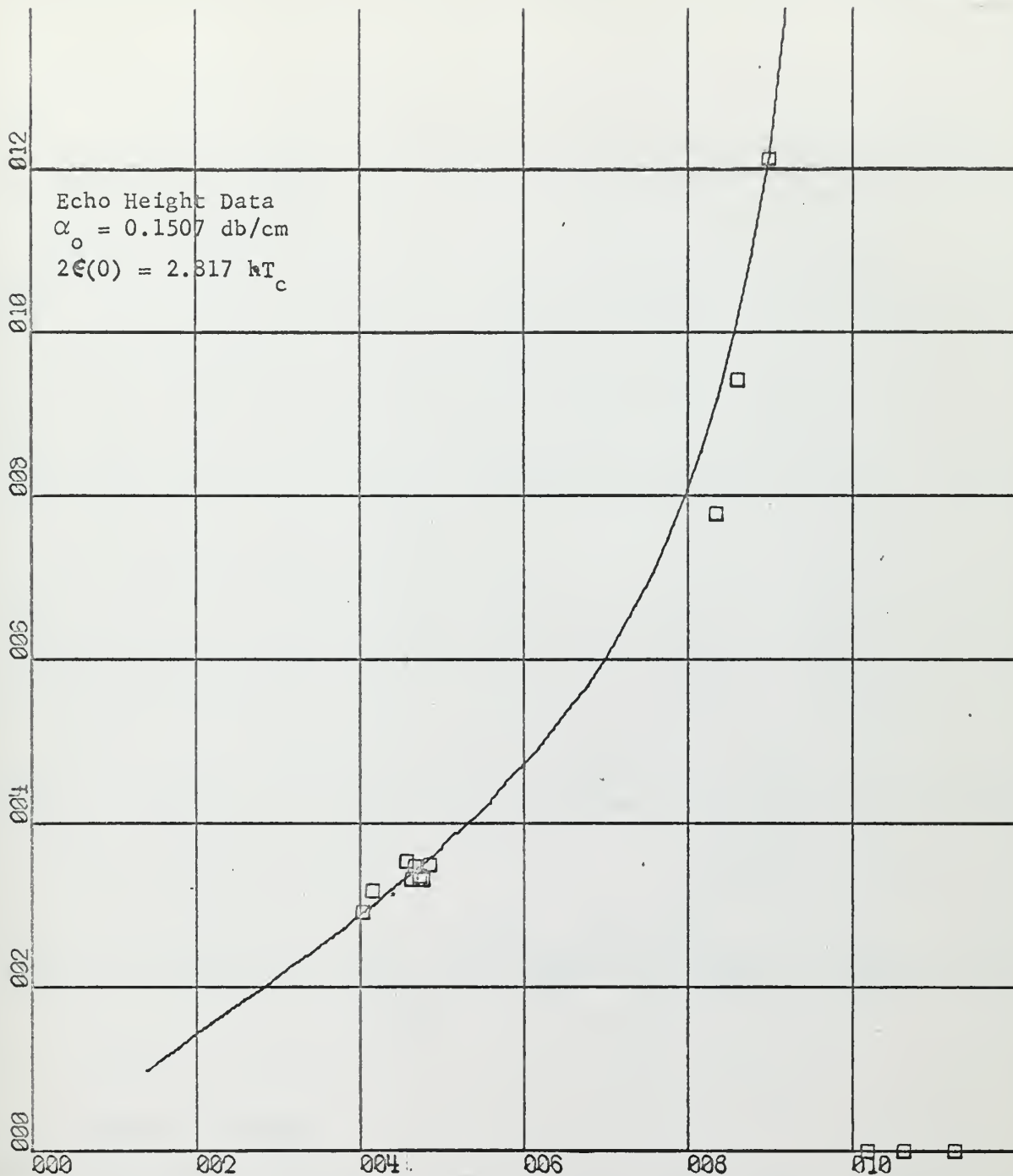
Fig. 16



X-SCALE = 2.00E-01 UNITS/INCH.
 Y-SCALE = 2.00E-01 UNITS/INCH.

GONCZ PROJECT 0321 13 NOV 64 30MCS.
 REDUCED ATTENUATION VS REDUCED TEMPERATURE

Fig. 17

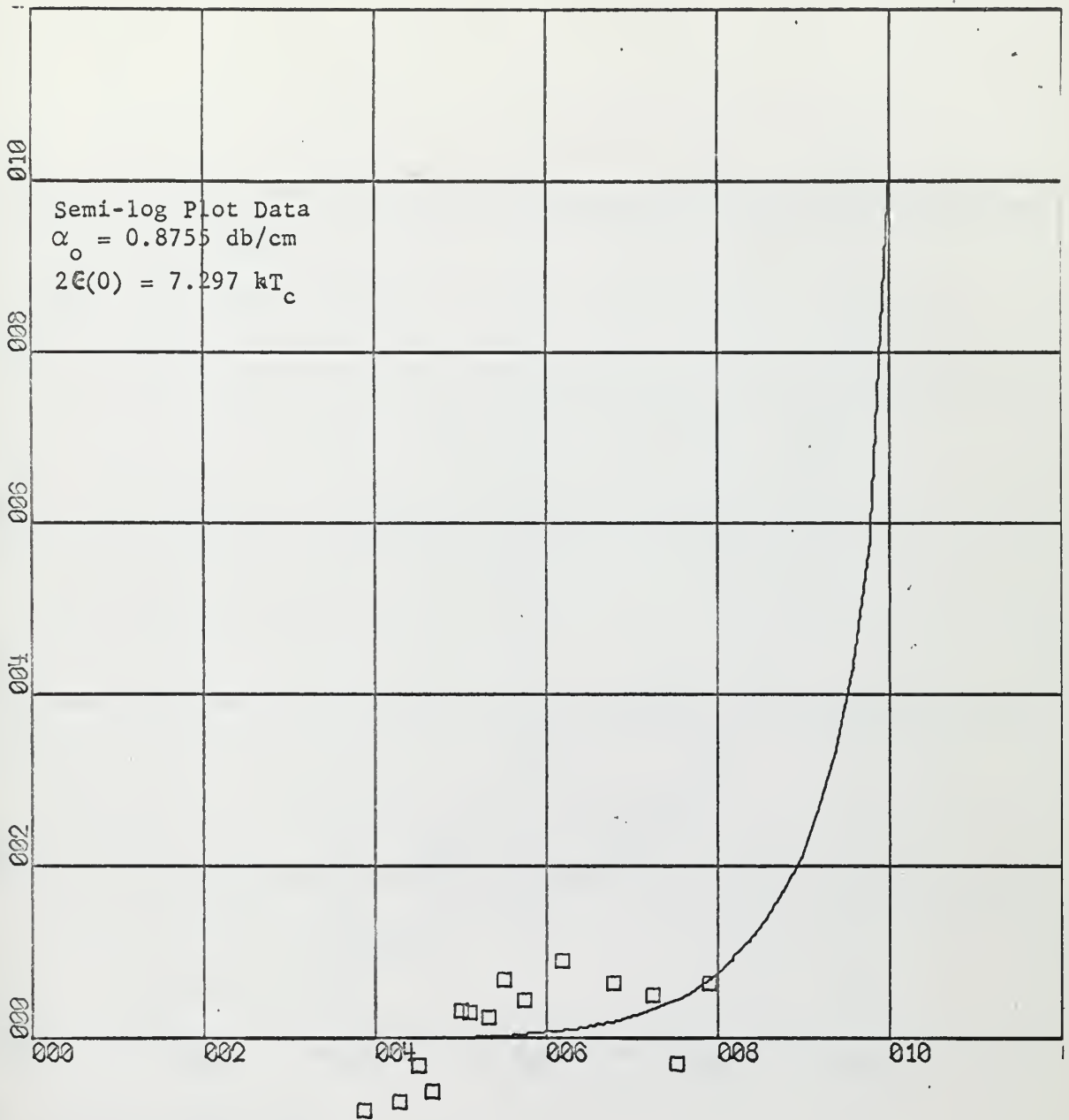


X-SCALE = 2.00E-01 UNITS/INCH.

Y-SCALE = 2.00E-01 UNITS/INCH.

GONCZ PROJECT 0321 13 NOV 64 30MCS
 $\gamma = 1 / (\log(2 / \alpha * - 1))$ VS REDUCED TEMPERATURE

Fig. 18

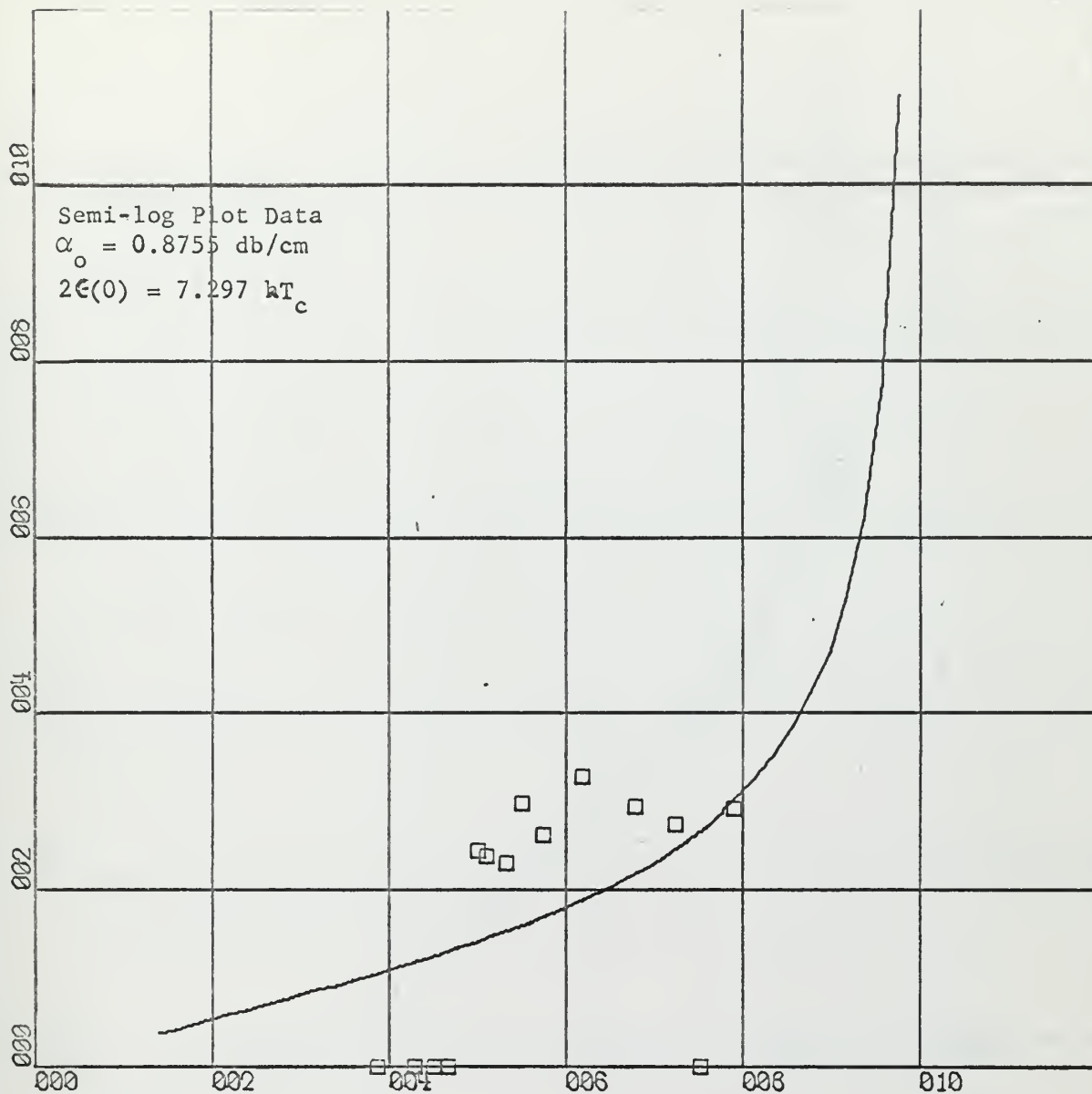


X-SCALE = $2.00E-01$ UNITS/INCH.
 Y-SCALE = $2.00E-01$ UNITS/INCH.

GONCZ PROJECT 0321 5 JAN 65 30MCS
 REDUCED ATTENUATION VS REDUCED TEMPERATURE

Fig. 19





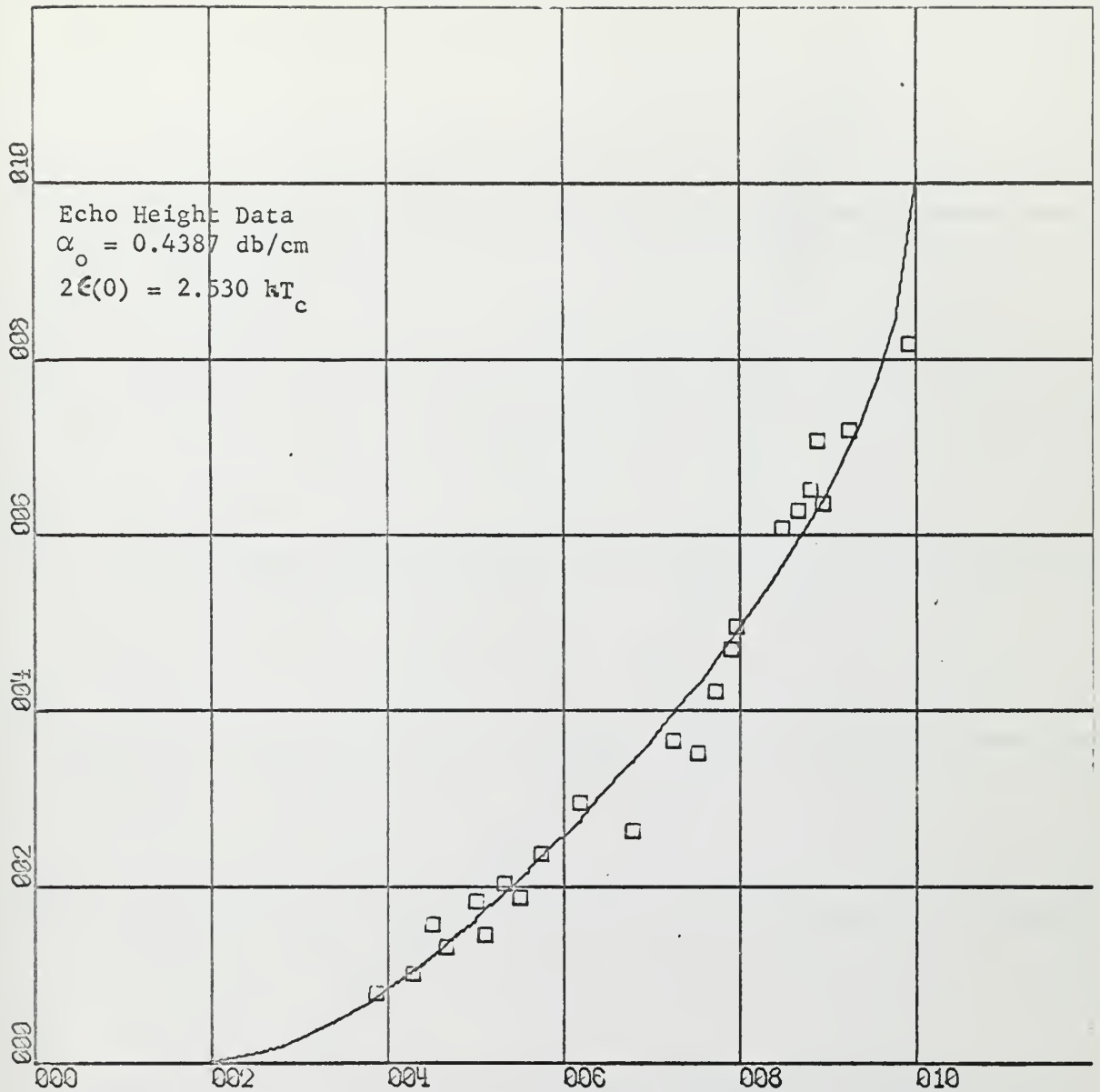
X-SCALE = 2.00E-01 UNITS/INCH.

Y-SCALE = 2.00E-01 UNITS/INCH.

GONCZ PROJECT 0321 5 JAN 65 30MCS

$\gamma = 1 / (\text{LOG}(2/\text{ALPHA} * -1))$ VS REDUCED TEMPERATURE

Fig. 20

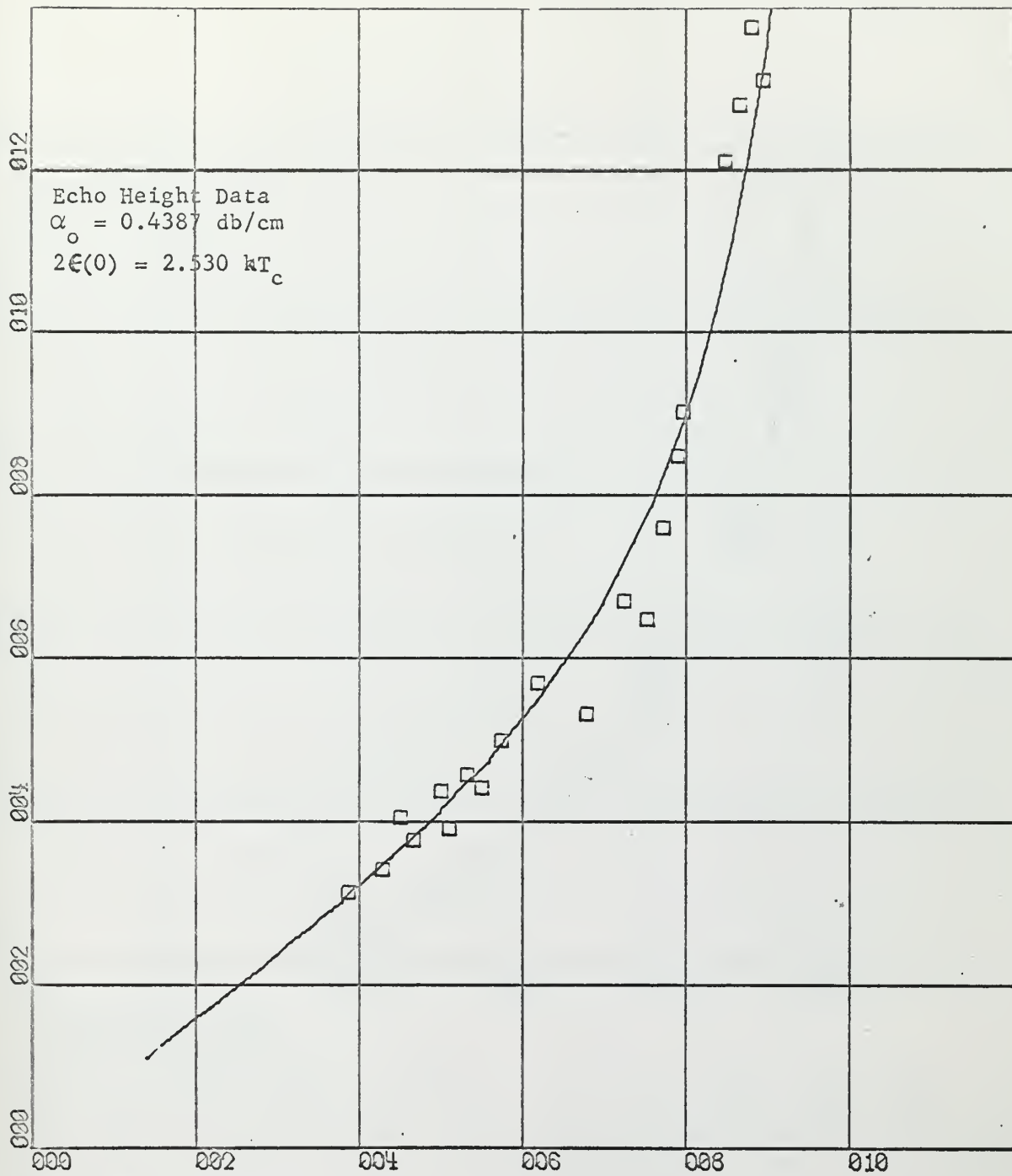


X-SCALE = 2.00E-01 UNITS/INCH.

Y-SCALE = 2.00E-01 UNITS/INCH.

GONCZ PROJECT 0321 5 JAN 65 30MCS
 REDUCED ATTENUATION VS REDUCED TEMPERATURE

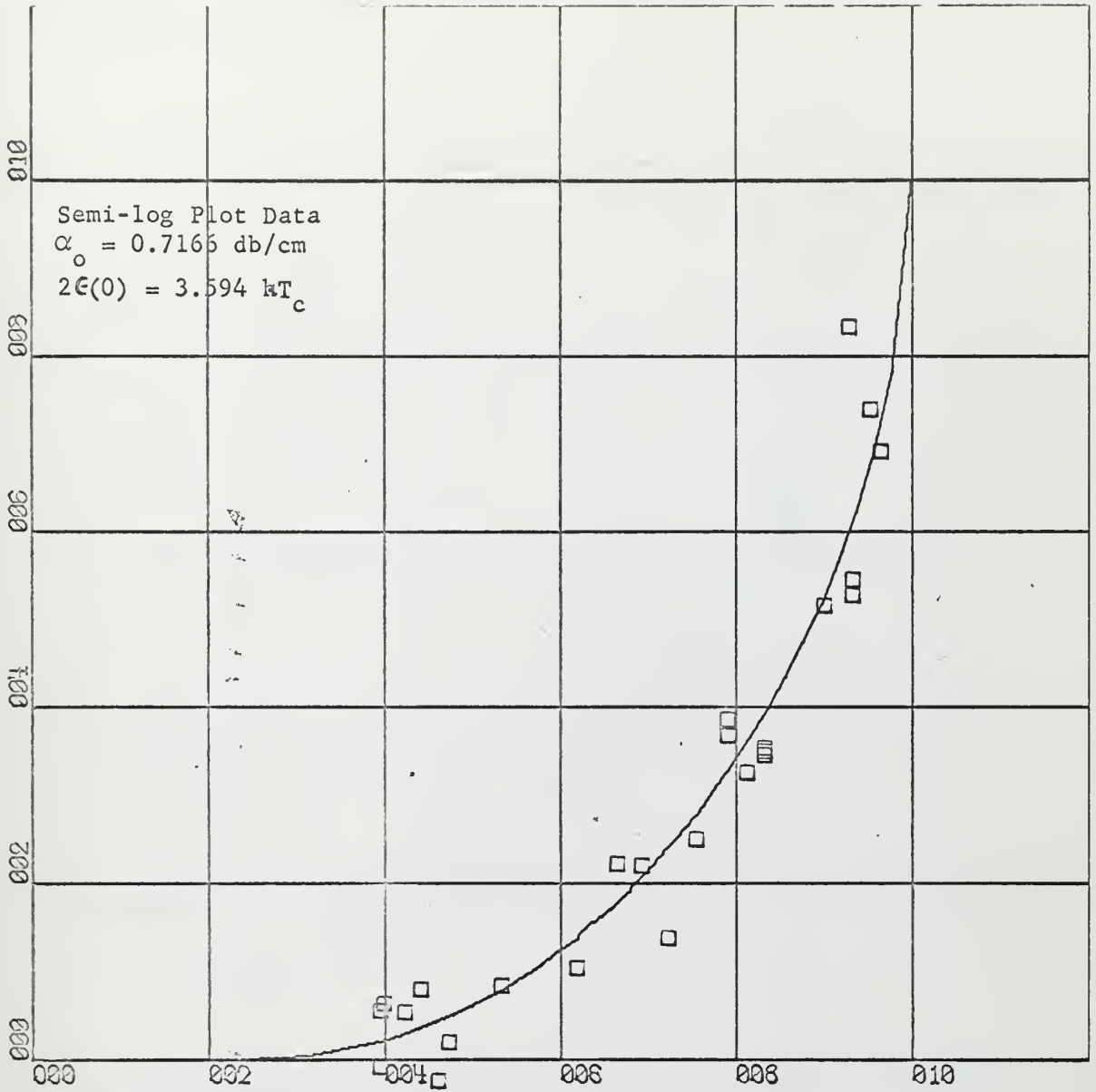
Fig. 21



X-SCALE = 2.00E-01 UNITS/INCH.
 Y-SCALE = 2.00E-01 UNITS/INCH.

GONCZ PROJECT 0321 5 JAN '65 30MCS
 $Y = 1 - (\text{LOG}(2/\text{ALPHA} * -1))$ VS REDUCED TEMPERATURE

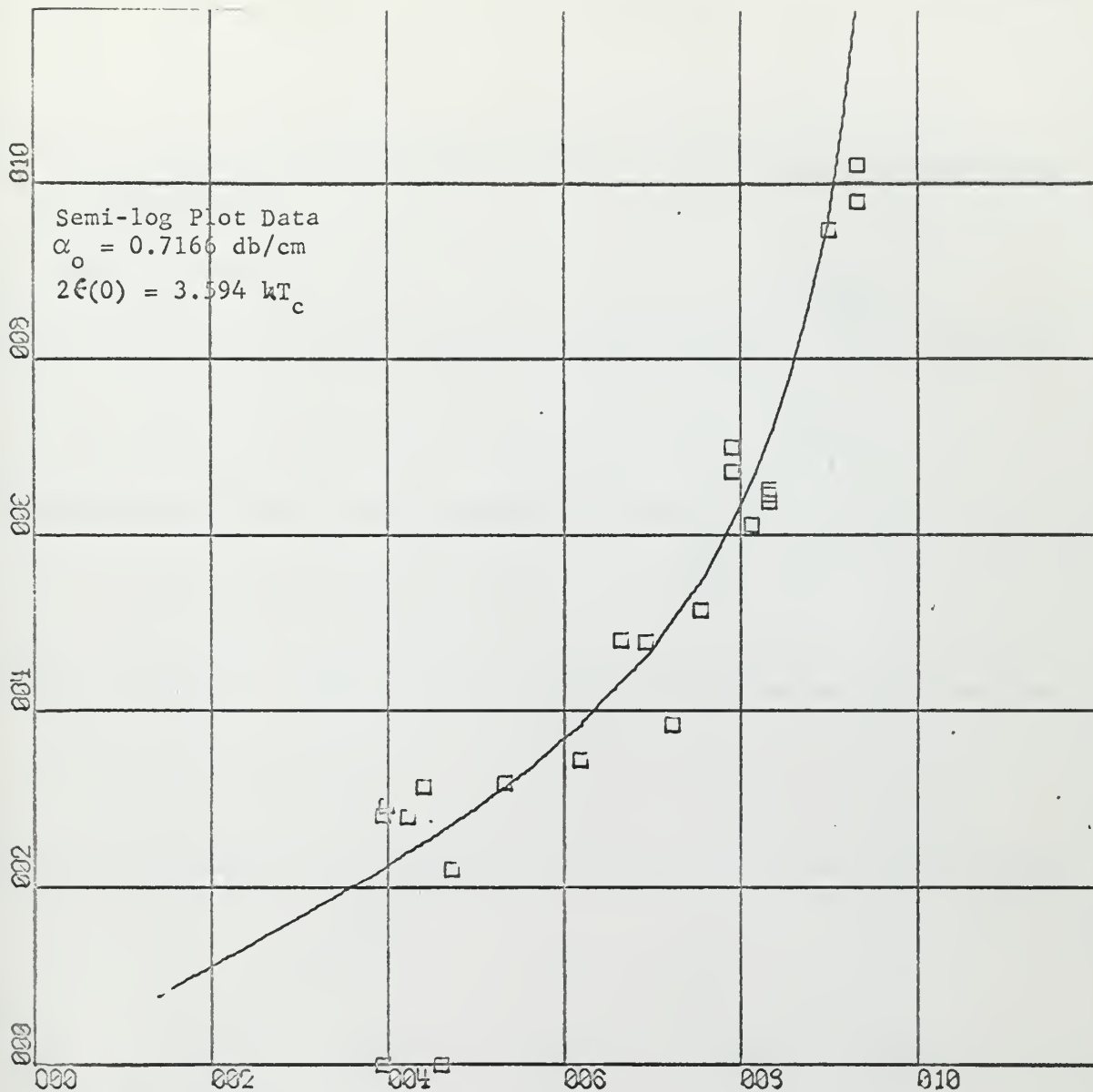
Fig. 22



X-SCALE = 2.00E-01 UNITS/INCH.
 Y-SCALE = 2.00E-01 UNITS/INCH.

GONCZ PROJECT 0321 5 JAN 65 10MCS
 REDUCED ATTENUATION VS REDUCED TEMPERATURE

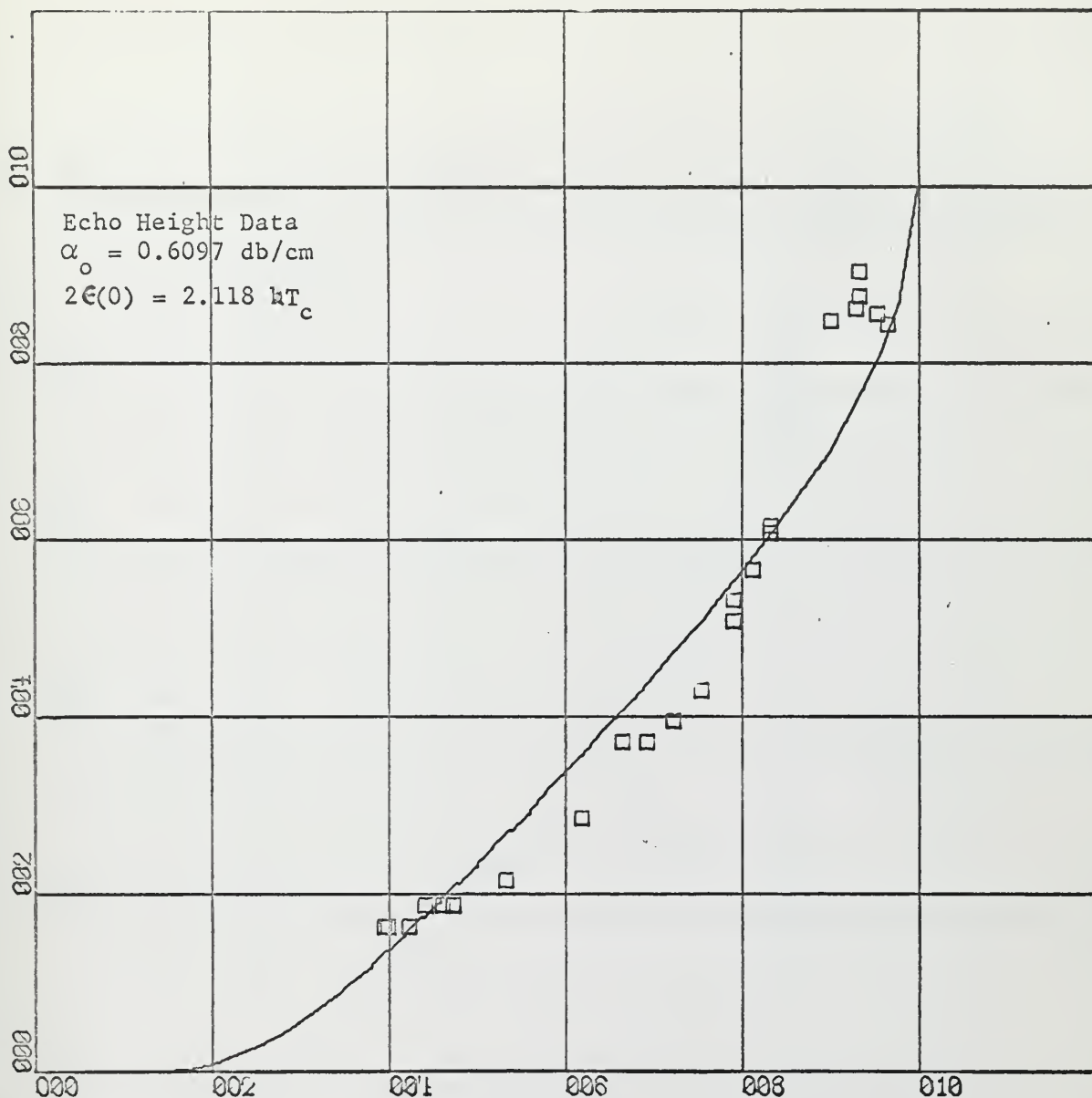
Fig. 23



X-SCALE = 2.00E-01 UNITS/INCH.
 Y-SCALE = 2.00E-01 UNITS/INCH.

GONCZ PROJECT 0321 5 JAN 65 10MCS
 $Y = 1 / (\text{LOG}(2 / \text{ALPHA} * - 1))$ VS REDUCED TEMPERATURE

Fig. 24

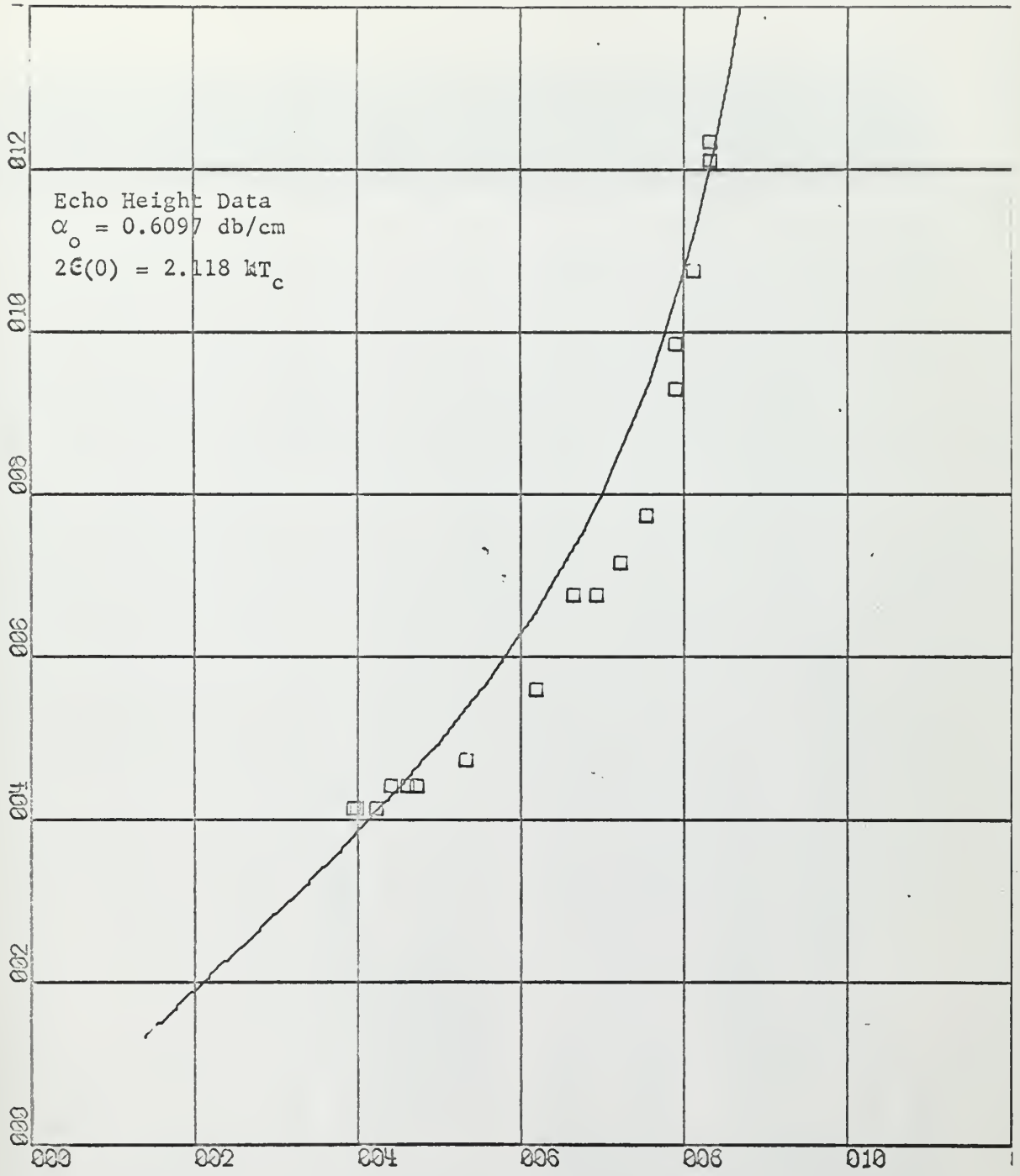


X-SCALE = 2.00E-01 UNITS/INCH.

Y-SCALE = 2.00E-01 UNITS/INCH.

GONCZ PROJECT 0321 5 JAN 65 10MCS
 REDUCED ATTENUATION VS REDUCED TEMPERATURE

Fig. 25



X-SCALE = 2.00E-01 UNITS/INCH.

Y-SCALE = 2.00E-01 UNITS/INCH.

GONCZ PROJECT 0321 5 JAN 65 10MCS

$Y = 1 - (\text{LOG}(2/\text{ALPHA} * -1))$ VS REDUCED TEMPERATURE

Fig. 26


```

00000000
00000010
00000020
00000030
00000040
00000050
00000060
00000070
00000080
00000090
00000100
00000110
00000120
00000130
00000140
00000150
00000160
00000170
00000180
00000190
00000200
00000210
00000220
00000230
00000240
00000250
00000260
00000270
00000280
00000290
00000300
00000310
00000320
00000330
00000340
00000350

..JOB0321F,GONCZ
PROGRAM ZEROGAP
DIMENSION US(1000),T(100),A(100),RT(100),UC(100),FER(100),ONE(100),TWO(100)
DO 1 I=1,100
  T(I)=0.
  A(I)=0.
  RT(I)=0.
  UC(I)=0.
  FER(I)=0.
  ONE(I)=0.
  TWO(I)=0.
1 DO 2 I=1,190
  US(I)=1.
  READ 3,(US(I),I=191,1000)
  3 FORMAT (10F7.0)
  READ 4,N,AN,TC,EGAP
  4 FORMAT (I10,3F10.0)
  READ 5,(I,(T(I),A(I)),J=1,N)
  5 FORMAT (I10,2F10.0)
  M=0
  DO 9 I=1,N
    RT(I)=T(I)/TC
    PT=RT(I)
    IF(PT)7,7,6
  6 IF(PT-1.)8,8,7
  7 UC(I)=0.
    M=M+1
  GO TO 9
  8 J=1000.*(PT+0.0005)
    UC(I)=US(J)/PT
  9 CONTINUE
  PRINT 10,(T(I),A(I),RT(I),UC(I),I=1,N)
  10 FORMAT (4E20.8)
  PX=EGAP
  TRY=EGAP-0.1

```



```

TEST=0.
DO 18 L=1,20
SUM1=0.
SUM2=0.
SUM3=0.
SUM4=0.
DO 14 I=1,N
PT=RT(I)
IF(PT)12,12,11
11 IF(PT-1.)13,13,12
12 FER(I)=0.
ONE(I)=0.
TWO(I)=0.
GO TO 14
13 FER(I)=1./(EXPF(UC(I)*PX/2.))+1.
ONE(I)=2.*FER(I)-1.
TWO(I)=2.*AN*FER(I)-A(I).
SUM1=SUM1+TWO(I)*ONE(I)
SUM2=SUM2+ONE(I)*ONE(I)
14 CONTINUE
AZ=SUM1/SUM2
DO 15 I=1,N
SUM3=SUM3+(TWO(I)-AZ*ONE(I))*UC(I)*FER(I)*(FER(I)-1.)*(AN-AZ)
SUM4=SUM4+(TWO(I)-AZ*ONE(I))*2
PRINT 16,L,PX,AZ,SUM4,SUM3
16 FORMAT (18H0
1 GAVE AZ=,F6.4,11H, RESIDUE=,1PE15.8,27H AND DERIVATIVE WRT EGA
2P=,1PE15.8)
IF(ABSF(SUM3)-1.E-07)19,17,17
17 TAN=PX-(PX-TRY)*SUM3/(SUM3-TEST)
TRY=PX
PX=TAN
18 TEST=SUM3
PX=TRY
19 PRINT 20,PX,AZ
20 FORMAT (82H0

```

BEST LEAST SQUARES FIT TO EXPERIMENTAL D00000710

00000360
00000370
00000380
00000390
00000400
00000410
00000420
00000430
00000440
00000450
00000460
00000470
00000480
00000490
00000500
00000510
00000520
00000530
00000540
00000550
00000560
00000570
00000580
00000590
00000600
00000610
00000620
00000630
00000640
00000650
00000660
00000670
00000680
00000690
00000700
00000710


```

DATA WAS ACHEIVED WITH EGAP=,F8.4,8H AND AZ=,F6.4)
COUNT=N-M
PER=SUM4/COUNT
PRINT 21,SUM4,PER
21 FORMAT (28H
1SIDUE PER EXPERIMENTAL VALUE USED IN THE FIT=,1PE15.8)
WITH RESIDUE=,1PE15.8,60H AND AVERAGE RE
STOP
END
END
00000720
00000730
00000740
00000750
00000760
00000770
00000780
00000790
00000800
00000810

```


99999 • 99998 • 99997 • 99996 • 99995 • 99994 • 99993 • 99992 • 99991 • 99990 • 200
 99987 • 99984 • 99982 • 99980 • 99978 • 99977 • 99975 • 99974 • 99974 • 99973 • 210
 99972 • 99972 • 99972 • 99972 • 99971 • 99971 • 99971 • 99971 • 99970 • 99970 • 220
 99970 • 99969 • 99968 • 99967 • 99966 • 99966 • 99965 • 99964 • 99963 • 99961 • 99960 • 230
 99958 • 99957 • 99955 • 99953 • 99951 • 99949 • 99947 • 99944 • 99942 • 99940 • 240
 99938 • 99935 • 99933 • 99931 • 99928 • 99926 • 99923 • 99921 • 99918 • 99916 • 250
 99913 • 99911 • 99908 • 99906 • 99903 • 99901 • 99898 • 99896 • 99893 • 99890 • 260
 99887 • 99884 • 99882 • 99879 • 99876 • 99872 • 99869 • 99866 • 99863 • 99859 • 270
 99856 • 99852 • 99848 • 99845 • 99841 • 99837 • 99833 • 99828 • 99824 • 99820 • 280
 99815 • 99811 • 99806 • 99801 • 99796 • 99791 • 99786 • 99781 • 99775 • 99770 • 290
 99764 • 99759 • 99753 • 99747 • 99742 • 99736 • 99730 • 99723 • 99717 • 99711 • 300
 99705 • 99698 • 99692 • 99685 • 99678 • 99672 • 99665 • 99658 • 99651 • 99644 • 310
 99636 • 99629 • 99622 • 99614 • 99607 • 99599 • 99592 • 99584 • 99576 • 99568 • 320
 99560 • 99551 • 99543 • 99535 • 99526 • 99518 • 99509 • 99500 • 99491 • 99482 • 330
 99473 • 99463 • 99454 • 99444 • 99434 • 99424 • 99414 • 99404 • 99394 • 99384 • 340
 99373 • 99362 • 99352 • 99341 • 99330 • 99318 • 99307 • 99295 • 99284 • 99272 • 350
 99260 • 99248 • 99236 • 99223 • 99211 • 99198 • 99185 • 99172 • 99159 • 99146 • 360
 99133 • 99119 • 99105 • 99092 • 99078 • 99064 • 99049 • 99035 • 99021 • 99006 • 370
 98991 • 98976 • 98961 • 98946 • 98931 • 98915 • 98900 • 98884 • 98868 • 98852 • 380
 98836 • 98820 • 98803 • 98787 • 98770 • 98753 • 98736 • 98719 • 98702 • 98684 • 390
 98667 • 98649 • 98631 • 98613 • 98595 • 98576 • 98558 • 98539 • 98520 • 98501 • 400
 98482 • 98463 • 98443 • 98424 • 98404 • 98384 • 98364 • 98344 • 98323 • 98303 • 410
 98282 • 98261 • 98240 • 98218 • 98197 • 98175 • 98153 • 98131 • 98109 • 98087 • 420
 98064 • 98041 • 98019 • 97995 • 97972 • 97949 • 97925 • 97901 • 97877 • 97853 • 430
 97829 • 97804 • 97780 • 97755 • 97730 • 97704 • 97679 • 97653 • 97627 • 97601 • 440
 97575 • 97549 • 97522 • 97496 • 97469 • 97441 • 97414 • 97387 • 97359 • 97331 • 450
 97303 • 97275 • 97246 • 97218 • 97189 • 97160 • 97131 • 97102 • 97072 • 97042 • 460
 97012 • 96982 • 96952 • 96921 • 96891 • 96860 • 96829 • 96798 • 96766 • 96734 • 470
 96703 • 96671 • 96638 • 96606 • 96573 • 96540 • 96507 • 96474 • 96441 • 96407 • 480
 96373 • 96339 • 96305 • 96270 • 96236 • 96201 • 96166 • 96130 • 96095 • 96059 • 490
 96023 • 95987 • 95950 • 95914 • 95877 • 95840 • 95803 • 95765 • 95728 • 95690 • 500
 95652 • 95613 • 95575 • 95536 • 95497 • 95458 • 95418 • 95378 • 95338 • 95298 • 510
 95258 • 95217 • 95176 • 95135 • 95094 • 95053 • 95011 • 94969 • 94927 • 94884 • 520
 94841 • 94798 • 94755 • 94712 • 94668 • 94624 • 94580 • 94536 • 94491 • 94447 • 530
 94402 • 94356 • 94311 • 94265 • 94219 • 94173 • 94127 • 94080 • 94033 • 93986 • 540
 93938 • 93891 • 93843 • 93795 • 93746 • 93698 • 93649 • 93600 • 93551 • 93501 • 550

• 93451 • 93401 • 93351 • 93300 • 93250 • 93199 • 93147 • 93096 • 93044 • 92992 • 560
 • 92940 • 92887 • 92835 • 92782 • 92728 • 92675 • 92621 • 92567 • 92513 • 92458 • 570
 • 92404 • 92349 • 92293 • 92238 • 92182 • 92126 • 92070 • 92013 • 91956 • 91899 • 580
 • 91842 • 91784 • 91726 • 91668 • 91610 • 91551 • 91492 • 91433 • 91373 • 91314 • 590
 • 91254 • 91193 • 91133 • 91072 • 91011 • 90949 • 90888 • 90826 • 90763 • 90701 • 600
 • 90638 • 90575 • 90512 • 90448 • 90384 • 90320 • 90255 • 90190 • 90125 • 90060 • 610
 • 89994 • 89928 • 89862 • 89795 • 89729 • 89661 • 89594 • 89526 • 89458 • 89390 • 620
 • 89321 • 89252 • 89183 • 89113 • 89043 • 88973 • 88903 • 88832 • 88761 • 88690 • 630
 • 88618 • 88546 • 88474 • 88401 • 88328 • 88255 • 88181 • 88107 • 88033 • 87959 • 640
 • 87884 • 87809 • 87733 • 87658 • 87582 • 87505 • 87428 • 87351 • 87274 • 87196 • 650
 • 87118 • 87040 • 86961 • 86882 • 86803 • 86723 • 86643 • 86563 • 86482 • 86401 • 660
 • 86320 • 86238 • 86156 • 86074 • 85992 • 85909 • 85825 • 85742 • 85658 • 85573 • 670
 • 85488 • 85403 • 85318 • 85232 • 85146 • 85060 • 84973 • 84886 • 84798 • 84711 • 680
 • 84622 • 84534 • 84445 • 84356 • 84266 • 84176 • 84086 • 83995 • 83904 • 83812 • 690
 • 83721 • 83628 • 83536 • 83443 • 83350 • 83256 • 83162 • 83068 • 82973 • 82878 • 700
 • 82782 • 82686 • 82590 • 82493 • 82396 • 82299 • 82201 • 82102 • 82004 • 81905 • 710
 • 81805 • 81706 • 81605 • 81505 • 81404 • 81302 • 81200 • 81098 • 80995 • 80892 • 720
 • 80789 • 80685 • 80580 • 80476 • 80370 • 80265 • 80159 • 80052 • 79945 • 79838 • 730
 • 79730 • 79622 • 79513 • 79404 • 79294 • 79184 • 79074 • 78963 • 78851 • 78739 • 740
 • 78627 • 78514 • 78401 • 78287 • 78173 • 78058 • 77943 • 77827 • 77711 • 77594 • 750
 • 77477 • 77359 • 77241 • 77122 • 77003 • 76884 • 76764 • 76643 • 76522 • 76400 • 760
 • 76278 • 76155 • 76032 • 75909 • 75784 • 75660 • 75535 • 75409 • 75283 • 75156 • 770
 • 75028 • 74901 • 74772 • 74644 • 74514 • 74384 • 74254 • 74123 • 73991 • 73859 • 780
 • 73727 • 73594 • 73460 • 73326 • 73191 • 73056 • 72920 • 72783 • 72646 • 72509 • 790
 • 72371 • 72232 • 72093 • 71953 • 71813 • 71672 • 71530 • 71388 • 71245 • 71102 • 800
 • 70958 • 70813 • 70668 • 70522 • 70375 • 70228 • 70081 • 69932 • 69783 • 69633 • 810
 • 69483 • 69332 • 69180 • 69028 • 68875 • 68721 • 68566 • 68411 • 68255 • 68098 • 820
 • 67941 • 67783 • 67624 • 67464 • 67303 • 67142 • 66980 • 66817 • 66654 • 66489 • 830
 • 66324 • 66158 • 65992 • 65824 • 65656 • 65486 • 65316 • 65146 • 64974 • 64801 • 840
 • 64628 • 64454 • 64279 • 64103 • 63926 • 63749 • 63570 • 63391 • 63210 • 63029 • 850
 • 62847 • 62665 • 62481 • 62296 • 62111 • 61924 • 61737 • 61549 • 61359 • 61169 • 860
 • 60978 • 60786 • 60593 • 60399 • 60204 • 60008 • 59811 • 59613 • 59414 • 59214 • 870
 • 59013 • 58810 • 58607 • 58402 • 58197 • 57990 • 57782 • 57572 • 57362 • 57150 • 880
 • 56937 • 56723 • 56508 • 56291 • 56073 • 55853 • 55632 • 55410 • 55186 • 54961 • 890
 • 54735 • 54507 • 54278 • 54047 • 53814 • 53580 • 53345 • 53108 • 52870 • 52630 • 900
 • 52388 • 52145 • 51901 • 51655 • 51407 • 51157 • 50907 • 50654 • 50400 • 50144 • 910

• 49886	• 49627	• 49366	• 49104	• 48839	• 48573	• 48305	• 48036	• 47764	• 47490	920
• 47214	• 46936	• 46656	• 46374	• 46090	• 45803	• 45513	• 45221	• 44926	• 44629	930
• 44329	• 44025	• 43719	• 43409	• 43096	• 42780	• 42460	• 42137	• 41810	• 41480	940
• 41146	• 40808	• 40466	• 40121	• 39772	• 39419	• 39063	• 38703	• 38340	• 37973	950
• 37603	• 37231	• 36855	• 36477	• 36096	• 35713	• 35328	• 34941	• 34551	• 34160	960
• 33767	• 33371	• 32973	• 32571	• 32166	• 31757	• 31342	• 30920	• 30490	• 30049	970
• 29595	• 29127	• 28639	• 28130	• 27595	• 27029	• 26429	• 25787	• 25100	• 24360	980
• 23562	• 22700	• 21767	• 20758	• 19667	• 18491	• 17228	• 15877	• 14440	• 12923	990
• 11338	• 09700	• 08034	• 06372	• 04757	• 03247	• 01913	• 00847	• 00163	• 00000	1000

APPENDIX V
PROGRAM AVERGAP

This program provides for a least squares fit to the BCS function using one parameter; the zero degree energy gap with the residual attenuation specified. Thus the program and the program notes are the same as those of Program Zero-gap, except that the residual attenuation is part of the input data rather than being derived from an analytic expression. The program will compute the zero degree energy gap which minimizes the square of the vertical distance from the experimental points to the BCS curve for three different values of residual attenuation. Thus, the expression

$$\sum_{i=1}^N \left[(2ANFER(I) - A(I)) - AZ(2FER(I) - 1) \right] UC \left[FER(FER-1) \right] [AN-AZ]$$

is minimized for each given AZ.

The type of data cards, their format, and order of input are the same as for Program Zerogap, with the exception that one card need be added. This is the last card and contains the three values of residual attenuation; the last digit of each to end in column 10, 20, and 30 respectively. These values are to be determined as in Program Resatt; i.e., from an extrapolation to $T = 0$ on a plot of the experimental data of attenuation vs temperature.

Table IV gives the results of Program Avergap and also a summary of all the computer calculations. It is seen that the results of Avergap are more consistent with those of Resatt than are those of Zerogap and again reflect the fact that the experimental points for higher t lie above the BCS curves used in Resatt. The results for the data of 5 Jan 65, 30 Mcs/sec still seem unreliable with such a high energy gap. This is due to the fact that there are data points for low t only.

RUN	FREQUENCY Mcs/sec	RESATT		AVERGAP		ZEROGAP	
		RESIDUAL ATTENUATION db/cm	ENERGY GAP $2\epsilon(0)/kT_c$	RESIDUAL ATTENUATION db/cm	ENERGY GAP $2\epsilon(0)/kT_c$	RESIDUAL ATTENUATION db/cm	ENERGY GAP $2\epsilon(0)/kT_c$

Attenuation from Semi-Log Plots

13 Nov 64	30	0.310	3.46	0.310	3.1560	0.1772	2.8544
		0.320	3.58	0.320	3.1797		
		0.330	3.62	0.330	3.2035		
5 Jan 65	30	0.525	2.96	0.525	3.7460	0.8755	7.2968
		0.565	3.26	0.565	3.9450		
		0.605	3.49	0.605	4.1707		
5 Jan 65	10	0.660	2.73	0.660	3.0940	0.7166	3.5941
		0.700	3.25	0.700	3.4380		
		0.740	3.63	0.740	3.8294		

Attenuation from Comparison of Echo Heights

13 Nov 64	30	0.290	3.45	0.290	3.1201	0.1507	2.8171
		0.300	3.58	0.300	3.1427		
		0.310	3.65	0.310	3.1654		
5 Jan 65	30	0.525	2.75	0.525	2.6598	0.4387	2.5304
		0.565	2.99	0.565	2.7237		
		0.605	3.57	0.605	2.7901		
5 Jan 65	10	0.700	3.01	0.700	2.5790	0.6097	2.1181
		0.715	3.23	0.715	2.6698		
		0.730	4.29	0.730	2.7649		

See Table I for experimental results

TABLE IV. SUMMARY OF COMPUTER CALCULATIONS


```

..JOB0321F,GONCZ
PROGRAM AVERGAP
DIMENSION US(1000),T(100),A(100),RT(100),UC(100),FER(100),ONE(100)
1,TWO(100),AZ(3)
DO 1 I=1,100
T(I)=0.
A(I)=0.
RT(I)=0.
UC(I)=0.
FER(I)=0.
ONE(I)=0.
1 TWO(I)=0.
DO 2 I=1,190
2 US(I)=1.
3 READ 3,(US(I),I=191,1000)
3 FORMAT (10F7.0)
4 READ 4,N,AN,TC,EGAP
4. FORMAT (I10,3F10.0)
5 READ 5,(I,(T(I),A(I)),J=1,N)
5 FORMAT (I10,2F10.0)
30 READ 30,AZ
30 FORMAT (3F10.0)
M=0
DO 9 I=1,N
RT(I)=T(I)/TC
PT=RT(I)
IF(PT)7,7,6
6 IF(PT-1.)8,8,7
7 UC(I)=0.
M=M+1
GO TO 9
8 J=1000.*(PT+0.0005)
UC(I)=US(J)/PT
9 CONTINUE
PRINT 10,(T(I),A(I),RT(I),UC(I),I=1,N)
10 FORMAT (4E20.8)
000000
000010
000020
000030
000040
000050
000060
000070
000080
000090
000100
000110
000120
000130
000140
000150
000160
000170
000180
000190
000200
000210
000220
000230
000240
000250
000260
000270
000280
000290
000300
000310
000320
000330
000340
000350

```



```

000360 DO 31 K=1,3
000370 PX=EGAP
000380 TRY=EGAP-0.1
000390 TEST=0.
000400 DO 18 L=1,20
000410 SUM3=0.
000420 SUM4=0.
000430 DO 14 I=1,N
000440 PT=RT(I)
000450 IF(PT)12,12,11
000460 11 IF(PT-1.)13,13,12
000470 12 FER(I)=0.
000480 ONE(I)=0.
000490 TWO(I)=0.
000500 GO TO 14
000510 13 FER(I)=1./((EXPF(UC(I)*PX/2.))+1.)
000520 ONE(I)=2.*FER(I)-1.
000530 TWO(I)=2.*AN*FER(I)-A(I)
000540 14 CONTINUE
000550 DO 15 I=1,N
000560 SUM3=SUM3+(TWO(I)-AZ(K)*ONE(I))*UC(I)*FER(I)*FER(I)-1.)*(AN-AZ(K)
000570 1)
000580 15 SUM4=SUM4+(TWO(I)-AZ(K)*ONE(I))*2
000590 PRINT 16,L,AZ(K),PX,SUM4,SUM3
000600 16 FORMAT (18H0 TRIAL NO,I3,10H WITH AZ=,F6.4/20H G
000610 1AVE EGAP=,F7.4,11H, RESIDUE=,1PE15.8,27H, AND DERIVITIVE WRT EGA
000620 2P=,1PE15.8)
000630 IF(ABSF(SUM3)-1.E-07)19,17,17
000640 17 TAN=PX-(PX-TRY)*SUM3/(SUM3-TEST)
000650 TRY=PX
000660 PX=TAN
000670 18 TEST=SUM3
000680 PX=TRY
000690 19 PRINT 20,AZ(K),PX
000700 20 FORMAT (68H0 BEST LEAST SQUARES FIT TO EXPERIMENTAL D
000710 1ATA WITH AZ=,F6.4,25H WAS ACHIEVED WITH EGAP=,F8.4,5H AND)

```



```
000720
000730
000740
000750
000760
000770
000780
000790

COUNT=N-M
PER=SUM4/COUNT
31 PRINT 21,SUM4,PER
21 FORMAT (28H
1 SIDUE PER EXPERIMENTAL VALUE USED IN THE FIT=,1PE15.8)
WITH RESIDUE=,1PE15.8,60H AND AVERAGE RE
STOP
END
END
```


99999 • 99998 • 99997 • 99996 • 99995 • 99994 • 99993 • 99992 • 99991 • 99990 • 200
 99987 • 99984 • 99982 • 99980 • 99978 • 99977 • 99975 • 99974 • 99974 • 99973 • 210
 99972 • 99972 • 99972 • 99972 • 99971 • 99971 • 99971 • 99971 • 99971 • 99970 • 99970 • 220
 99970 • 99969 • 99968 • 99967 • 99966 • 99965 • 99964 • 99963 • 99961 • 99960 • 230
 99958 • 99957 • 99955 • 99953 • 99951 • 99949 • 99947 • 99944 • 99942 • 99940 • 240
 99938 • 99935 • 99933 • 99931 • 99928 • 99926 • 99923 • 99921 • 99918 • 99916 • 250
 99913 • 99911 • 99908 • 99906 • 99903 • 99901 • 99898 • 99896 • 99893 • 99890 • 260
 99887 • 99884 • 99882 • 99879 • 99876 • 99872 • 99869 • 99866 • 99863 • 99859 • 270
 99856 • 99852 • 99848 • 99845 • 99841 • 99837 • 99833 • 99828 • 99824 • 99820 • 280
 99815 • 99811 • 99806 • 99801 • 99796 • 99791 • 99786 • 99781 • 99775 • 99770 • 290
 99764 • 99759 • 99753 • 99747 • 99742 • 99736 • 99730 • 99723 • 99717 • 99711 • 300
 99705 • 99698 • 99692 • 99685 • 99678 • 99672 • 99665 • 99658 • 99651 • 99644 • 310
 99636 • 99629 • 99622 • 99614 • 99607 • 99599 • 99592 • 99584 • 99576 • 99568 • 320
 99560 • 99551 • 99543 • 99535 • 99526 • 99518 • 99509 • 99500 • 99491 • 99482 • 330
 99473 • 99463 • 99454 • 99444 • 99434 • 99424 • 99414 • 99404 • 99394 • 99384 • 340
 99373 • 99362 • 99352 • 99341 • 99330 • 99318 • 99307 • 99295 • 99284 • 99272 • 350
 99260 • 99248 • 99236 • 99223 • 99211 • 99198 • 99185 • 99172 • 99159 • 99146 • 360
 99133 • 99119 • 99105 • 99092 • 99078 • 99064 • 99049 • 99035 • 99021 • 99006 • 370
 98991 • 98976 • 98961 • 98946 • 98931 • 98915 • 98900 • 98884 • 98868 • 98852 • 380
 98836 • 98820 • 98803 • 98787 • 98770 • 98753 • 98736 • 98719 • 98702 • 98684 • 390
 98667 • 98649 • 98631 • 98613 • 98595 • 98576 • 98558 • 98539 • 98520 • 98501 • 400
 98482 • 98463 • 98443 • 98424 • 98404 • 98384 • 98364 • 98344 • 98323 • 98303 • 410
 98282 • 98261 • 98240 • 98218 • 98197 • 98175 • 98153 • 98131 • 98109 • 98087 • 420
 98064 • 98041 • 98019 • 97995 • 97972 • 97949 • 97925 • 97901 • 97877 • 97853 • 430
 97829 • 97804 • 97780 • 97755 • 97730 • 97704 • 97679 • 97653 • 97627 • 97601 • 440
 97575 • 97549 • 97522 • 97496 • 97469 • 97441 • 97414 • 97387 • 97359 • 97331 • 450
 97303 • 97275 • 97246 • 97218 • 97189 • 97160 • 97131 • 97102 • 97072 • 97042 • 460
 97012 • 96982 • 96952 • 96921 • 96891 • 96860 • 96829 • 96798 • 96766 • 96734 • 470
 96703 • 96671 • 96638 • 96606 • 96573 • 96540 • 96507 • 96474 • 96441 • 96407 • 480
 96373 • 96339 • 96305 • 96270 • 96236 • 96201 • 96166 • 96130 • 96095 • 96059 • 490
 96023 • 95987 • 95950 • 95914 • 95877 • 95840 • 95803 • 95765 • 95728 • 95690 • 500
 95652 • 95613 • 95575 • 95536 • 95497 • 95458 • 95418 • 95378 • 95338 • 95298 • 510
 95258 • 95217 • 95176 • 95135 • 95094 • 95053 • 95011 • 94969 • 94927 • 94884 • 520
 94841 • 94798 • 94755 • 94712 • 94668 • 94624 • 94580 • 94536 • 94491 • 94447 • 530
 94402 • 94356 • 94311 • 94265 • 94219 • 94173 • 94127 • 94080 • 94033 • 93986 • 540
 93938 • 93891 • 93843 • 93795 • 93746 • 93698 • 93649 • 93600 • 93551 • 93501 • 550

• 93451 • 93401 • 93351 • 93300 • 93250 • 93199 • 93147 • 93096 • 93044 • 92992 • 560
 • 92940 • 92887 • 92835 • 92782 • 92728 • 92675 • 92621 • 92567 • 92513 • 92458 • 570
 • 92404 • 92349 • 92293 • 92238 • 92182 • 92126 • 92070 • 92013 • 91956 • 91899 • 580
 • 91842 • 91784 • 91726 • 91668 • 91610 • 91551 • 91492 • 91433 • 91373 • 91314 • 590
 • 91254 • 91193 • 91133 • 91072 • 91011 • 90949 • 90888 • 90826 • 90763 • 90701 • 600
 • 90638 • 90575 • 90512 • 90448 • 90384 • 90320 • 90255 • 90190 • 90125 • 90060 • 610
 • 89994 • 89928 • 89862 • 89795 • 89729 • 89661 • 89594 • 89526 • 89458 • 89390 • 620
 • 89321 • 89252 • 89183 • 89113 • 89043 • 88973 • 88903 • 88832 • 88761 • 88690 • 630
 • 88618 • 88546 • 88474 • 88401 • 88328 • 88255 • 88181 • 88107 • 88033 • 87959 • 640
 • 87884 • 87809 • 87733 • 87658 • 87582 • 87505 • 87428 • 87351 • 87274 • 87196 • 650
 • 87118 • 87040 • 86961 • 86882 • 86803 • 86723 • 86643 • 86563 • 86482 • 86401 • 660
 • 86320 • 86238 • 86156 • 86074 • 85992 • 85909 • 85825 • 85742 • 85658 • 85573 • 670
 • 85488 • 85403 • 85318 • 85232 • 85146 • 85060 • 84973 • 84886 • 84798 • 84711 • 680
 • 84622 • 84534 • 84445 • 84356 • 84266 • 84176 • 84086 • 83995 • 83904 • 83812 • 690
 • 83721 • 83628 • 83536 • 83443 • 83350 • 83256 • 83162 • 83068 • 82973 • 82878 • 700
 • 82782 • 82686 • 82590 • 82493 • 82396 • 82299 • 82201 • 82102 • 82004 • 81905 • 710
 • 81805 • 81706 • 81605 • 81505 • 81404 • 81302 • 81200 • 81098 • 80995 • 80892 • 720
 • 80789 • 80685 • 80580 • 80476 • 80370 • 80265 • 80159 • 80052 • 79945 • 79838 • 730
 • 79730 • 79622 • 79513 • 79404 • 79294 • 79184 • 79074 • 78963 • 78851 • 78739 • 740
 • 78627 • 78514 • 78401 • 78287 • 78173 • 78058 • 77943 • 77827 • 77711 • 77594 • 750
 • 77477 • 77359 • 77241 • 77122 • 77003 • 76884 • 76764 • 76643 • 76522 • 76400 • 760
 • 76278 • 76155 • 76032 • 75909 • 75784 • 75660 • 75535 • 75409 • 75283 • 75156 • 770
 • 75028 • 74901 • 74772 • 74644 • 74514 • 74384 • 74254 • 74123 • 73991 • 73859 • 780
 • 73727 • 73594 • 73460 • 73326 • 73191 • 73056 • 72920 • 72783 • 72646 • 72509 • 790
 • 72371 • 72232 • 72093 • 71953 • 71813 • 71672 • 71530 • 71388 • 71245 • 71102 • 800
 • 70958 • 70813 • 70668 • 70522 • 70375 • 70228 • 70081 • 69932 • 69783 • 69633 • 810
 • 69483 • 69332 • 69180 • 69028 • 68875 • 68721 • 68566 • 68411 • 68255 • 68098 • 820
 • 67941 • 67783 • 67624 • 67464 • 67303 • 67142 • 66980 • 66817 • 66654 • 66489 • 830
 • 66324 • 66158 • 65992 • 65824 • 65656 • 65486 • 65316 • 65146 • 64974 • 64801 • 840
 • 64628 • 64454 • 64279 • 64103 • 63926 • 63749 • 63570 • 63391 • 63210 • 63029 • 850
 • 62847 • 62665 • 62481 • 62296 • 62111 • 61924 • 61737 • 61549 • 61359 • 61169 • 860
 • 60978 • 60786 • 60593 • 60399 • 60204 • 60008 • 59811 • 59613 • 59414 • 59214 • 870
 • 59013 • 58810 • 58607 • 58402 • 58197 • 57990 • 57782 • 57572 • 57362 • 57150 • 880
 • 56937 • 56723 • 56508 • 56291 • 56073 • 55853 • 55632 • 55410 • 55186 • 54961 • 890
 • 54735 • 54507 • 54278 • 54047 • 53814 • 53580 • 53345 • 53108 • 52870 • 52630 • 900
 • 52388 • 52145 • 51901 • 51655 • 51407 • 51157 • 50907 • 50654 • 50400 • 50144 • 910

• 49886	• 49627	• 49366	• 49104	• 48839	• 48573	• 48305	• 48036	• 47764	• 47490	920
• 47214	• 46936	• 46656	• 46374	• 46090	• 45803	• 45513	• 45221	• 44926	• 44629	930
• 44329	• 44025	• 43719	• 43409	• 43096	• 42780	• 42460	• 42137	• 41810	• 41480	940
• 41146	• 40808	• 40466	• 40121	• 39772	• 39419	• 39063	• 38703	• 38340	• 37973	950
• 37603	• 37231	• 36855	• 36477	• 36096	• 35713	• 35328	• 34941	• 34551	• 34160	960
• 33767	• 33371	• 32973	• 32571	• 32166	• 31757	• 31342	• 30920	• 30490	• 30049	970
• 29595	• 29127	• 28639	• 28130	• 27595	• 27029	• 26429	• 25787	• 25100	• 24360	980
• 23562	• 22700	• 21767	• 20758	• 19667	• 18491	• 17228	• 15877	• 14440	• 12923	990
• 11338	• 09700	• 08034	• 06372	• 04757	• 03247	• 01913	• 00847	• 00163	• 00000	1000

REFERENCES

1. H.E. Bömmel, Phys. Rev. 96, 220 (1954).
2. L. Mackinnon, Phys. Rev. 98, 1181, 1210 (1955).
3. J. Bardeen, L.N. Cooper, and J.R. Schrieffer, Phys. Rev. 108, 1175 (1957).
4. R.W. Morse and H.V. Bohm, Phys. Rev. 108, 1094 (1957).
5. For a general review of Ultrasonic Attenuation in Metals at Low Temperatures, see R.W. Morse, Progress in Cryogenics, edited by K. Mendelssohn (Heywood & Co., Ltd., London, 1959), Vol. I, p. 219.
6. For a general review of the Superconducting Energy Gap, see D.H. Douglass Jr., and L.M. Falicov, Progress in Low Temperature Physics, edited by C.J. Gorter (North-Holland Publishing Co., Amsterdam, 1964), Vol. IV, p. 97.
7. R.W. Morse, T. Olsen, and J.D. Gavenda, Phys. Rev. Ltrs. 3, 15 (1959).
8. J.G. Daunt and D.O. Edwards, Temperature - Its Measurement and Control in Science & Industry (Reinhold Publishing Corp., New York, 1962), Vol. 3, Part I.
9. N.E. Phillips, Phys. Rev. Ltrs. 1, 363 (1958).
10. T.H. Geballe and B.T. Matthias, IBM J. Research Develop. 6, 256 (1962).
11. J.F. Cochran and D.E. Mapother, Phys. Rev. 121, 1688 (1961).
12. H.V. Bohm and N.H. Horowitz, Proceedings of the Eighth International Conference on Low Temperature Physics, edited by R.O. Davies (Butterworths, London, 1963), p. 191.
13. M.A. Biondi, M.P. Garfunkel, and W.A. Thompson, Phys. Rev. 136, A1471 (1964).
14. S. Zemon and H.A. Boorse, Bull. Am. Phys. Soc. 9, 268, (1964).
15. R. Weber, Phys. Rev. 133, A1487 (1964).
16. G.A. Saunders and W.A. Lawson, Phys. Rev. 135, A1161 (1964).
17. V.M. Bobetic, Phys. Rev. 136, A1535 (1964).
18. B. Mühlischlegel, Z. Phys. 155, 313 (1959).

thesG547

Ultrasonic attenuation in superconductin



3 2768 002 13090 8

DUDLEY KNOX LIBRARY